Fungal Genetics and Biology 159 (2022) 103656

Contents lists available at ScienceDirect

Fungal Genetics and Biology

journal homepage: www.elsevier.com/locate/yfgbi

Candida glabrata Hst1-Rfm1-Sum1 complex evolved to control virulence-related genes

Norma Vázquez-Franco [a], Guadalupe Gutiérrez-Escobedo [a], Alejandro Juárez-Reyes [a], Emmanuel Orta-Zavalza [b], Irene Castaño [a], Alejandro De Las Peñas [a,*]

[a] IPICYT, División de Biología Molecular, Instituto Potosino de Investigación Científica y Tecnológica, Camino a la Presa San José, #2055, Col. Lomas 4ª Sección, San Luis Potosí, San Luis Potosí 78216, Mexico
[b] Departamento de Ciencias Químico-Biológicas, Universidad Autónoma de Ciudad Juárez, Chihuahua, Mexico

ARTICLE INFO

Keywords:
Candida glabrata
Hst1
Sum1
Rfm1
Pdr1
Cdr1
Fluconazole

ABSTRACT

C. glabrata is an opportunistic fungal pathogen and the second most common cause of opportunistic fungal infections in humans, that has evolved virulence factors to become a successful pathogen: strong resistance to oxidative stress, capable to adhere and form biofilms in human epithelial cells as well as to abiotic surfaces and high resistance to xenobiotics. Hst1 (a NAD^+-dependent histone deacetylase), Sum1 (putative DNA binding protein) and Rfm1 (connector protein) form a complex (HRS-C) and control the resistance to oxidative stress, to xenobiotics (the antifungal fluconazole), and adherence to epithelial cells. Hst1 is functionally conserved within the *Saccharomycetaceae* family, Rfm1 shows a close phylogenetic relation within the *Saccharomycetaceae* family while Sum1 displays a distant phylogenetic relation with members of the family and is not conserved functionally. *CDR1* encodes for an ABC transporter (resistance to fluconazole) negatively controlled by HRS-C, for which its binding site is located within 223 bp upstream from the ATG of *CDR1*. The absence of Hst1 and Sum1 renders the cells hyper-adherent, possibly due to the overexpression of *AED1*, *EPA1*, *EPA22* and *EPA6*, all encoding for adhesins. Finally, in a neutrophil survival assay, *HST1* and *SUM1*, are not required for survival. We propose that Sum1 in the HRS-C diverged functionally to control a set of genes implicated in virulence: adherence, resistance to xenobiotics and oxidative stress.

1. Introduction

To establish a successful infection within the host, microbial pathogens must be capable of evading the host's immune response and rapidly adjust to the new environment. For colonization and persistence, pathogens have evolved virulence factors to detect and respond to the new conditions: a robust oxidative stress response to evade and survive the attack of phagocytic cells, adherence to host epithelial cells and biofilm formation and recently, resistance to human designed antifungal drugs.

Candida glabrata is the second most common cause of opportunistic fungal infections in humans and *C. glabrata* infections have increased in the last decade (Pfaller et al., 2014). As other pathogens, *C. glabrata* has also evolved virulence factors to avoid host defenses and favor a successful infection. For example: multidrug resistance (Orta-Zavalza et al., 2013; Sanglard et al., 1999), a strong resistance to oxidative stress (Cuéllar-Cruz et al., 2008; Roetzer et al., 2011, 2010), the ability to evade killing by macrophages (Seider et al., 2011), adherence to host epithelial cells and biofilm formation (Castaño et al., 2005; Cormack et al., 1999; Redding et al., 2003; Timmermans et al., 2018). The expression of these virulence factors is tightly regulated according to the changing environment within the host.

The multidrug resistance in *C. glabrata* is controlled by the transcription factor Pdr1 that induces the expression of the ABC transporter genes (*CDR1* and *CDR2*, among others) (reviewed in Ferrari et al., 2009; Morschhäuser, 2010; Moye-Rowley, 2019; Whaley and Rogers, 2016). Pdr1 is activated in the presence of the antifungal fluconazole (FLC) by the direct binding of FLC to the Pdr1 xenobiotic binding domain (XBD) (Thakur et al., 2008). Activated Pdr1 induces the expression of the ABC transporters that extrude FLC out of the cell (Lamping et al., 2010; Vermitsky et al., 2006). The oxidative stress response in *C. glabrata* is regulated by the transcription factors Yap1, Skn7, Msn2 and Msn4. In the presence of oxidative stress, these transcription factors positively control the expression of genes encoding antioxidant enzymes such as superoxide dismutases (*SOD1* and *SOD2*), catalase (*CTA1*), sulfiredoxin

* Corresponding author.
E-mail address: cano@ipicyt.edu.mx (A. De Las Peñas).

https://doi.org/10.1016/j.fgb.2021.103656
Received 2 September 2020; Received in revised form 25 December 2021; Accepted 27 December 2021
Available online 30 December 2021

Table 1
Strains used in this work.

Escherichia coli strain		
Strain	Genotype	Reference
DH10	F⁻ *mcrA* Δ (*mrr-hsdRMS-mcrBC*) F80 Δ*lacZ* Δ*M*15 Δ*lacX74 deoR recA1 endA1 araD*139 Δ (*ara,leu*)*7697 galU galK* l⁻ *rpsL nupG*	(Calvin and Hanawalt, 1988)

Saccharomyces cerevisiae and *Lachancea kluyveri* strains		
Strain	Genotype	Reference
Saccharomyces cerevisiae	*MATα his3Δ 1, leu2Δ 0, lys2Δ 0, ura3Δ 0*	(Brachmann, 1998)
Lachancea kluyveri	Wild type NRRL Y-12651	(Kurtzman, 2003)

Candida glabrata strains			
Strain	Parental	Genotype	Reference
BG2	Clinical Isolate		(Cormack and Falkow, 1999)
BG14	BG2	*ura*3Δ::Tn*903* G418^R	(Cormack et al., 1999)
BG676 *sir*3 Δ	BG14	*ura*3Δ::Tn*903* G418^R *sir*3 Δ	(De Las Peñas et al., 2003)
CGM84 *hst*1Δ	BG1073	*ura*3Δ::Tn*903* G418^R *hst*1Δ	(Orta-Zavalza et al., 2013)
CGM673 *sum*1Δ	BG14	*ura*3Δ::Tn*903* G418^R *sum*1Δ::*hph* Hyg^R	(Orta-Zavalza et al., 2013)
BG1073 *hst*1Δ	BG14	*ura*3Δ::Tn*903* G418^R *hst*1Δ::*hph* Hyg^R	(Domergue et al., 2005)
CGM1094 *pdr*1Δ	BG14	*ura*3Δ::Tn*903* G418^R *pdr*1Δ::*hph* Hyg^R	(Orta-Zavalza et al., 2013)
CGM1232 *sum*1Δ	CGM673	*ura*3Δ::Tn*903* G418^R *sum*1Δ	(Orta-Zavalza et al., 2013)
CGM1605	CGM84	*ura*3Δ::Tn*903* G418^R *HST1* reconstituted	(Orta-Zavalza et al., 2013)
CGM1611	CGM1232	*ura*3Δ::Tn*903* G418^R *SUM1* reconstituted	(Orta-Zavalza et al., 2013)
CGM943	BG14	*ura*3Δ::Tn*903* G418^R *rfm*1Δ::*NatMX4* Nat^R	(Orta-Zavalza et al., 2013)
CGM1234 *rfm*1Δ	CGM943	*ura*3Δ::Tn*903* G418^R *rfm*1Δ	(Orta-Zavalza et al., 2013)
Strains for heterologous complementation			
CGM3148	CGM1232	*ura*3Δ::Tn*903* G418^R *sum*1Δ::*LkSUM1*	This work
CGM3192	CGM1232	*ura*3Δ::Tn*903* G418^R *sum*1Δ::*ScSUM1*	This work
CGM3935	CGM84	*ura*3Δ::Tn*903* G418^R *hst*1Δ::*ScHST1*	This work
Strains carrying plasmids with GFP transcriptional fusions			
CGM514	BG14	*ura*3Δ::Tn*903* G418^R pMC14 (pGFP::3′UTR$_{CTA1}$)	(Gutiérrez-Escobedo et al., 2020)
CGM3756	BG14	*ura*3Δ::Tn*903* G418^R *CDR1*::pP$_{CDR1}$::GFP::3′UTR$_{CDR1}$	This work
CGM3758	CGM84 ***hst1Δ***	*ura*3Δ::Tn*903* G418^R *CDR1*::pP$_{CDR1}$::GFP:: 3′UTR$_{CDR1}$ *hst*1Δ	This work
CGM3760 *sum*1Δ	CGM1232	*ura*3Δ::Tn*903* G418^R *CDR1*::pP$_{CDR1}$::GFP::3′UTR$_{CDR1}$ *sum*1Δ	This work
CGM3778 *pdr*1Δ	CGM1094	*ura*3Δ::Tn*903* G418^R *CDR1*::pP$_{CDR1}$::GFP::3′UTR$_{CDR1}$ *pdr*1Δ	This work
CGM1923	BG14	*ura*3Δ::Tn*903* G418^R pCV37 (pP$_{CDR1}$::GFP:: 3′UTR$_{CDR1}$) Ura$^+$	(Gutiérrez-Escobedo et al., 2020)
CGM4067 *rfm*1Δ	CGM1234	*ura*3Δ::Tn*903* G418^R *CDR1*::pP$_{CDR1}$::GFP::3′UTR$_{CDR1}$ *rfm*1Δ clone 1	This work
CGM4068 *rfm*1Δ	CGM1234	*ura*3Δ::Tn*903* G418^R *CDR1*::pP$_{CDR1}$::GFP::3′UTR$_{CDR1}$ *rfm*1Δ clone 2	This work
CGM4069 *rfm*1Δ	CGM1234	*ura*3Δ::Tn*903* G418^R *CDR1*::pP$_{CDR1}$::GFP::3′UTR$_{CDR1}$ *rfm*1Δ clone 3	This work
Strains tagged with FLAG or cMyc			
CGM934	CGM823	*ura*3Δ::Tn*903* G418^R *HST1-cMyc13*	(Orta-Zavalza et al., 2013)
CGM982	CGM934	*ura*3Δ::Tn*903* G418^R *HST1-cMyc13 SUM1-FLAG::hph* Hyg^R	(Orta-Zavalza et al., 2013)
CGM1294	CGM982	*ura*3Δ::Tn*903* G418^R *HST1-cMyc13 SUM1-FLAG::hph* Hyg^R *rfm*1Δ::*NatMX4* Nat^R	(Orta-Zavalza et al., 2013)
CGM1340	BG14	*ura*3Δ::Tn*903* G418^R *SUM1-FLAG::hph* Hyg^R	(Orta-Zavalza et al., 2013)

(*SRX1*) and peroxiredoxins (*TSA1* and *TSA2*), as well as the synthesis of glutathione and thioredoxin (Briones-Martin-del-Campo et al., 2015; Cuéllar-Cruz et al., 2008; Gutiérrez-Escobedo et al., 2020, 2013; Juárez-Cepeda et al., 2015; Roetzer et al., 2011; Saijo et al., 2010; Seider et al., 2014). Adherence to host epithelial cells is mediated by cell wall proteins encoded by the *EPA* gene family. Almost all *EPA* genes are located at subtelomeric regions and their expression is negatively controlled by chromatin-based subtelomeric silencing. Subtelomeric silencing depends on the activity of NAD^+-dependent histone deacetylase Sir2, the founder member of the sirtuins (Cormack et al., 1999; De Las Peñas et al., 2003; Domergue et al., 2005). Interestingly, *EPA1* is activated by Pdr1 carrying a gain of function mutation (Vale-Silva et al., 2013, 2016), *EPA2* is induced by Yap1 and Skn7 in the presence of oxidative stress (Juárez-Cepeda et al., 2015) and *EPA6*, *EPA20*, *EPA22* are negatively controlled by Hst1 a NAD^+-dependent histone deacetylase (Domergue et al., 2005; Ma et al., 2009). Given that Hst1 is inactive in the absence of NAD^+, Hst1 regulates its own activity by controlling the expression of genes encoding high affinity niacin (precursor of NAD^+) transporters (*TNA1*, *TNR1* and *TNR2*), required to maintain homeostasis of NAD^+ in the cell, thus controlling indirectly the expression of almost all *EPA* genes under subtelomeric silencing (Ma et al., 2009). In addition, Hst1 negatively controls the expression of *PDR1* and *CDR1* for multidrug resistance and of *MSN4* and *CTA1* for oxidative stress (Orta-Zavalza et al., 2013). Consistent with the genetic analysis Hst1, Sum1 (putative DNA binding protein) and Rfm1 (connector protein) physically interact forming a complex (HRS-C) (Orta-Zavalza et al., 2013).

C. glabrata is closely related phylogenetically to the non-pathogenic yeast *Saccharomyces cerevisiae* and has been classified in the genus *Nakaseomyces* within the *glabrata* group (Gabaldón et al., 2013). In spite of their phylogenetic relationship, there are clear specific genetic differences (Herrero, 2005). For example, *C. glabrata* compared to *S. cerevisiae* is highly resistant to oxidative stress and to xenobiotics and is capable to adhere to human epithelial cells. In particular, the HRS-C in *S. cerevisiae* negatively controls the expression of mid-sporulation genes (MMG) during vegetative growth. Even though Sum1 DNA binding domain has not been described, it has been proposed that Sum1 binds to the MME (medium meiosis element), *cis* elements present in the MMG promoters, recruits Hst1 and prevents the access of the transcription activator Ndt80 (Piekarska et al., 2010). Sum1 is inactivated by phosphorylation dependent on the kinase Ime2 (Pak and Segall, 2002). Despite *C. glabrata* not having a sexual cycle, with no meiosis or sporulation, Hst1 controls the expression of orthologous genes implicated in mid-sporulation (Ma et al., 2009). Interestingly, Hst1 also controls the response to oxidative stress, multidrug resistance and adherence, genes implicated in virulence (Ma et al., 2009; Orta-Zavalza et al., 2013). These data suggest that the *Cg*HRS-C could be a central regulator of

Table 2
Plasmids used in this study.

Plasmid	Relevant genotype	Reference
Cloning vectors		
pRS306	pBluescript, *URA3*	(Sikorski and Hieter, 1989)
pMB11	Cloning vector *sacB* counterselection Cm^R *ori* p15A	(Briones-Martin-del-Campo et al., 2015; Gallegos-Garcia et al., 2012)
pAP668	GFP cloned in pRS306 for transcriptional fusions. *URA3* Integrative vector Ap^R	(Gutiérrez-Escobedo et al., 2020)
Plasmids for heterologous complementation		
pVF27	A 4.87 kb *BamH* I/*Sal* I PCR fusion fragment (primers 859/860) carrying the promoter (0.83 kb PCR fragment, primers 859/1006) and 3′UTR (0.84 kb PCR fragment, primers 1009/860) of *CgSUM1*, and *ScSUM1* ORF (3.19 kb PCR fragment, primers 1007/1008) cloned in pRS306 [pP_{SUM1}::*ScSUM1*::$3'UTR_{SUM1}$]. *URA3 CgCEN ARS* Ap^R	This work
pVF31	A 4.37 kb *BamH* I/*Sal* I PCR fusion fragment (primers 859/860) carrying the promoter (0.83 kb PCR fragment, primers 859/1012) and 3′UTR (0.84 kb PCR fragment, primers 1015/860) of *CgSUM1*, and *LkSUM1* ORF (2.70 kb PCR fragment, primers 1013/1014) cloned in pRS306 [pP_{SUM1}::*LkSUM1*::$3'UTR_{SUM1}$]. *URA3 CgCEN ARS* Ap^R	This work
pVF73	A 3.32 kb *Sac* II/*Xho* I PCR fusion fragment (primers 2514/789) carrying the promoter (0.82 kb PCR fragment, primers 2514/2515) and 3′UTR (1.03 kb PCR fragment, primers 2516/789) of *CgSUM1*, and *ScHST1* ORF (1.51 kb, primers 2512/2513) cloned in pRS306 [pP_{HST1}::*ScHST1*::$3'UTR_{HST1}$]. *URA3 CgCEN ARS* Ap^R	This work
Plasmids for transcriptional fusions with GFP		
pCV37	Transcriptional fusion between *CTA1* and GFP [pP_{CTA1}::GFP::$3'UTR_{CTA1}$] *URA3 CgCEN ARS* Ap^R	(Gutiérrez-Escobedo et al., 2020)
pVF65	A 0.60 kb *Kpn* I/*Sal* I PCR fragment (primers 2494/2495) carrying the promoter and a 0.97 kb *BamH* I/*Sac* I PCR fragment (primers 2496/2497) carrying the 3′UTR of *CgCDR1* cloned in pAP668 [pP_{CDR1}::GFP::$3'UTR_{CDR1}$]. *URA3 CgCEN ARS* Ap^R	This work

stress response genes.

In this work, we show that Hst1 and Rfm1 are conserved within the *Saccharomycetaceae* family and are not present in the *Candida/Lodderomyces* clade. Sum1 shows a distant phylogenetic relationship between the *glabrata* group and other members of the *Saccharomycetaceae* family. Consistent with the phylogenetic analysis, *ScSUM1* does not complement *CgSUM1*. We propose that *Cg*Sum1 evolved to redirect the HRS-C to control an additional set of genes in *C. glabrata*. HRS-C negatively controls the expression of *CDR1* by binding within 223 bp upstream from the ATG of *CDR1*. *C. glabrata* cells lacking Hst1 and Sum1 become hyper-adherent possibly due to the overexpression of *AED1*, *EPA1*, *EPA22* and *EPA6*. Furthermore, in a neutrophil survival assay, neither *HST1* nor *SUM1* are required for survival. In summary, we show that the HRS-C diverged functionally to control a different set of genes implicated in virulence: adherence, resistance to xenobiotics and oxidative stress.

2. Materials and methods

2.1. Strains

All strains used in this study are described in Table 1.

2.2. Plasmids

All plasmids used in this work are described in Table 2.

2.3. Primers

All primers used in this study are described in Table 3.

2.4. Media and growth conditions

Yeast media were prepared as described previously (Gutiérrez-Escobedo et al., 2020). 2 % agar (Thermo Fisher Scientific™) was added for plates. **Y**east Extract-**P**eptone-**D**extrose (**YPD**) medium contained 10 g/L yeast extract, 20 g/L peptone (Thermo Fisher Scientific™) and glucose 2% (J.T.Baker®). **S**ynthetic **C**omplete medium (**SC**) contained yeast nitrogen base without $(NH_4)_2\ SO_4$ at 1.7 g/L, $(NH_4)_2\ SO_4$ at 5 g/L, 0.6 % casamino acids (BD - Difco™), 2% glucose and when needed supplemented with Fluconazol (Pfizer®). All yeast cultures were grown for 48 h at 30°C. Bacterial cultures were grown overnight at 30°C. Bacterial medium is **L**uria–**B**ertani medium (**LB**): 10 g/L NaCl (Sigma Aldrich®), 10 g/L peptone and 5 g/L yeast extract. LB media was supplemented with 1.5% agar for plates and if required with 50 μg/ml of carbenicillin (Invitrogen).

2.5. Plasmid construction

All fragments for plasmid constructs were generated by PCR and for the heterologous complementation experiments, fusion PCR was performed as previously described (Baudin et al., 1993) using genomic DNA from *S. cerevisiae* BY4742 or *L. kluyveri* NRRL Y-12651 as templates. All PCR products were purified before cloning using Qiagen® Gel Extraction Kit. For the *C. glabrata* heterologous complementation experiment with a) *HST1*, the intergenic region between *CgRTG1* and *CgHST1* containing the promoter of *CgHST1* was fused with *ScHST1* ORF and *CgHST1* 3′UTR and b) *SUM1*, the intergenic region between *CgTFB1* and *CgSUM1* containing the promoter of *CgSUM1* was fused with *ScSUM1* ORF or *LkSUM1* ORF and *CgSUM1* 3′UTR. All fragments were cloned in the integrative plasmid Prs306. Plasmids are as follows pP_{CgHST1}::*ScHST1*::$3'UTR_{CgHST1}$, pP_{CgSUM1}::*ScSUM1*::$3'UTR_{CgSUM1}$, and pP_{CgSUM1}::*LkSUM1*::$3'UTR_{CgSUM1}$. To construct the transcriptional fusion between GFP and *CDR1*, the fragments containing the intergenic region between *SPT7* and *CDR1* carrying the promoter of *CDR1* and the 3′UTR of *CDR1* were cloned in the integrative plasmid pAP668: pP_{CDR1}::GFP::$3'UTR_{CDR1}$. All plasmid constructs were introduced into *Escherichia coli* DH10 by electroporation (Ausubel, 1992). All plasmids were purified and sequenced from *E. coli* DH10 using the Qiagen® Plasmid Kit QIAprep.

2.6. Strain construction

The *hst*1Δ mutant strain was transformed with linearized pP_{CgHST1}::*ScHST1*::$3'UTR_{CgHST1}$ digested with *Hind* III site present in 3′UTR*CgHST1*. *sum*1Δ mutant strain was transformed with linearized pP_{CgSUM1}::*ScSUM1*::$3'UTR_{CgSUM1}$ digested with *Mfe* I site present in $3'UTR_{CgHST1}$ and linearized pP_{CgSUM1}::*LkSUM1*::$3'UTR_{CgSUM1}$ digested with *Pac* I site present in the P_{CgHST1}. BG14 parental strain, *hst*1Δ, *pdr*1Δ, *rfm*1Δ, and *sum*1Δ were transformed with linearized pP_{CDR1}::GFP::$3'UTR_{CDR1}$ digested with *BstE* II site present in the $3'UTR_{CDR1}$. All plasmids were integrated in their cognate site and verified with locus-specific genomic primers.

Table 3
Oligonucleotides used in this work.

No.	Sequence	Site
789	CGA**CTCGAG**TACGGTGCCGCTGTTC	*Xho* I
859	GAG**GGATCC**GGTACGTTAGCTGTGTGCG	*BamH* I
860	ACG**GTCGAC**AAACGTTCGCGCAGC	*Sal* I
1006	GTGGTGTTCTCAGACATAGCTGGTTTATATAATTGTTTCTAAGC	
1007	ATGTCTGAGAACACCACAGC	
1008	TAACGGATATCTGGCGGTATG	
1009	CCGCCAGATATCCGTTAAAACAACTCGTATATATAAGAGTCTCAATAC	
1012	ACAACATGGCTATCAACACTCATAGCTGGTTTATATAATTGTTTCTAAGC	
1013	ATGAGTGTTGATAGCCATGTTG	
1014	ACGAGTTGTTCTAAACCTCTGGTTG	
1015	CCTCAACCAGAGGTTTAGAACAACTCGTATATATAAGAGTCTCAATAC	
2494	CGG**GGTACC**CAGGACATAGATCAGAG	*Kpn* I
2495	CAAG**GTCGAC**TGTTACTTTTCTTTACTTTG	*Sal* I
2496	CGC**GGATCC**TTTATTTAGCCTGCGCTC	*BamH* I
2497	CAAG**GAGCTC**GATCTGAACGTAATTTCC	*Sac* I
2512	ATGAACATATTGCTAATGCAACGG	
2513	TTACTGTTGTTTCTTTCGTGGCTG	
2514	ACAC**CCGCGG**AGACGAAACGCAGG	*Sac* II
2515	TGCATTAGCAATATGTTCATTCCTAATTTCTTGGTCACCG	
2516	CACGAAAGAAACAACAGTAAACCGCTCATTTGTTTTTATAATAG	
2750	AGGCGAGTCTCTACATCTAACT	
2751	CCATAGGTTCCGTCCTTTCTG	
2764	ACAACCTTCGGACACGATAAG	
2765	GATCTTCTGTGCGTCTCTTCTT	
2770	AGAAACTGGACGAGGAAGTTAAG	
2771	TCACCACTGTTGCTGCTATT	
2910	TGGAAGAAAGACCATCGAATTA	
2911	GCACACACACAAACAAACAA	
2912	ATCCAAGTCCAGGTCCAA	
2913	CAGCTATGAGTTGAGGAAGATT	
2915	GAAGGATCAAGAATTCGATTACAAC	
2920	GGCATCCTTCTTGTCACTT	
2921	CAAACCCAGGACATAGATCAG	
2924	CATAGCTGCTAGAAGAAAGAGA	
2927	CCCAGTTGATGATGGTAAGG	
2928	CCATCTTTGTCGGTAGTAGTG	
2931	CAACAGCAGTGGAGAATACA	
2932	CGTCTTTGGTTTCCTTGATTAC	
2939	ACAGGCTATAAATCACACAGAC	
2940	TTGTCAATGGTGTACGATAGTT	
2949	CTGTTGCAGACAAGAGAGTAG	
2950	TCATGTCAAGGTACACAGTAAG	
2955	TTGCCAGCAGGTTACAATTA	
2956	GTGGATACCCGATGTTTGAG	
A16	CTTTCGGCAATACCTGGG	
A17	TCCTACGAACTTCCAGATGG	
H46	CATGGTATTGTTACCAACTGGG	
H47	AAGAGTATAGAGACAAGACGGC	

2.7. Yeast transformation

Yeast transformation was performed using the lithium acetate protocol as described previously (Castaño et al., 2003). All transformants were selected on SC-Ura plates and incubated at 30°C.

2.8. Phylogenetic and evolution analysis

The Hst1, Rfm1 and Sum1 orthologous sequences were searched in *Candida* Genome Database (http://www.candidagenome.org/, CGD Copyright © 2004–2017 The Board of Trustees, Leland Stanford Junior University; Skrzypek et al., 2017), Genome Resources for Yeast Chromosomes (http://gryc.inra.fr/; GRYC © INRA 2013–2015), PhylomeDB (http://phylomedb.org/; Comparative Genomics Group; Huerta-Cepas et al., 2011), Yeast Genome Order Browser (http://ygob.ucd.ie/, YGOB © Kevin Byrne-Wolfe Laboratory; Byrne and Wolfe, 2005), and NCBI (https://www.ncbi.nlm.nih.gov/, National Center for Biotechnology Information, U.S. National Library of Medicine). In addition, a BLAST search for similar sequences was made within the *Saccharomycetales*. Sequences were retrieved from 29 species (Table 4). The orthologous sequences were analyzed using ClustalW (Higgins et al., 1996; Larkin et al., 2007) and MUSCLE (Edgar, 2004) with MEGA v7 program (Kumar et al., 2016). All alignments were edited with PhyDE® (Phylogenetic Data Editor, http://www.phyde.de/) and analyzed with statistical selection of amino acids substitution models with ModelFinder (Kalyaanamoorthy et al., 2017) with AIC, corrected AIC and BIC criteria. Phylogenetic and molecular evolution analysis was done with MEGA v7 (Kumar et al., 2016) (*Neighbor-Joining method*) and IQ-TREE server (Maximum Likelihood) (Trifinopoulos et al., 2016). The *Neighbor-Joining* analysis was done with JTT substitution model with 1000 replication *bootstrap* and Gamma distribution. These results were used to perform the maximum likelihood analysis with the model substitution of LG + F + R5 (Hst1) and JTT + F + I + G4 (Rfm1 and Sum1) with *ultrafast bootstrap* of 1000 replications in agreement with the ModelFinder selection results (Minh et al., 2013). The percentage of identity and similarity of Hst1, Rfm1, and Sum1 between *C. glabrata* and *S. cerevisiae* was done by ClustalW alignment (Higgins et al., 1996; Larkin et al., 2007) with the MacVector program (Accelrys).

2.9. Fluconazole sensitivity assays

Sensitivity to Fluconazole (Pfizer®) was determined as described

Table 4
Access number or systematic name of sequences used in the phylogenetic analysis.

Clade	Specie	Hst1	Rfm1	Sum1
	Hanseniaspora opuntiae	OEJ85856	OEJ90056	OEJ83615
	Hanseniaspora uvarum	OEJ81758	OEJ87168	KKA03429
Candida/Lodderomyces	*Candida albicans*	C1_09050W_A	–	–
	Candida dubliniensis	Cd36_08540	–	–
	Candida tropicalis	CTRG_03242	–	–
	Candida orthopsilosis	CORT_0A03930	–	–
	Candida parapsilosis	CPAR2_803900	–	–
KLE	*Kluyveromyces lactis*	KLLA0F14663g	KLLA0C07062g	KLLA0C14696g
	Lachancea kluyveri	SAKL0C08602g	SAKL0H05060g	SAKL0G09460g
	Lachancea thermotolerans	KLTH0C08690g	KLTH0D12694g	KLTH0F07194g
	Lachancea waltii	Kwal_56.22853_s56	Kwal_26.9097-s26	Kwal_33.14342
	Eremothecium gossypii	AEL013C	AER355C	AAL045C
	Eremothecium cymbalariae	Ecym_5284	Ecym_6246	Ecym_3213
ZT	*Zygosaccharomyces bailii*	BN860_09846g1_1	SJM87887	SJM83795
	Zygosaccharomyces rouxii	ZYRO0B05148g	ZYRO0A06050g	ZYRO0C14146g
	Torulaspora delbrueckii	TDEL0D04710	TDEL0B03710	TDEL0E02930
WGD	*Vanderwaltozyma polyspora*	Kpol_479.29_s479	Kpol_413.10-s413	Kpol_1005.6
	Tetrapisispora phaffii	TPHA_0A00880	TPHA-0G01350	TPHA0D01960
	Naumovozyma castellii	NCAS0C03490	NCAS0B00560	NCAS0F02810
	Naumovozyma dairenensis	NDAI0G02830	NDAI0E00830	NDAI0C04270
	Kazachstania africana	KAFR0C01100	KAFR0A04190	KAFR0K02210
	Kazachstania naganishii	KNAG0K01070	KNAG0G02910	XP_022462891
	Saccharomyces cerevisiae	YOL068C	YOR279C	YDR310C
	Saccharomyces eubayanus	XM_018365469	DI49-5098	XP_018223852
	Saccharomyces kudriavzevii	SKUD_12120	SKUD_15.443	SKUD_4.573
glabrata group	*Candida glabrata*	CAGL0C05357g	CAGL0L11022g	CAGL0J10956g
	Candida bracarensis	CABR0s04e00341g1	CABR0s17e00803g	CABR0s16e01034g
	Candida nivariensis	CANI0s09e04664g1	CANI0s16e00792g	CANI0s15e01507g
	Nakaseomyces delphensis	NADE0s25e00286g1	NADE0s06e04411g	NADE0s13e01221g

previously (Orta-Zavalza et al., 2013). Cultures were grown for 48 h at 30°C in YPD, washed and resuspended in distilled water. The OD_{600nm} of all cultures were adjusted, serial dilutions were made and 5 μL spotted onto YPD plates containing different concentrations of Fluconazole. Cells were incubated at 30°C.

2.10. H_2O_2 sensitivity assays

Sensitivity to H_2O_2 of log phase cells was determined as described previously (Cuéllar-Cruz et al., 2008; Orta-Zavalza et al., 2013). A 35% H_2O_2 solution (Sigma Aldrich®) was used for the assay. Cultures were grown for 48 h at 30°C in YPD and diluted into fresh media. After 7 duplications, cells were exposed to H_2O_2 for 3 h. Cells were washed, resuspended in distilled water and their OD_{600nm} adjusted to 0.5. Cells were plated on YPD plates and incubated at 30°C.

2.11. Flow cytometry analysis of GFP expression

GFP expression experiments were done as described previously (Gutiérrez-Escobedo et al., 2020) with some modifications. Cells were grown in YPD. Samples were taken every 2 h and fluorescence was assessed by fluorescence activated cell sorter (FACS) using a FACSCalibur flow cytometer (BD Biosciences) with Cell Quest Pro software. GFP was used as reporter gene to measure the activity of the *CDR1* promoter. The negative control was the strain with a promoterless GFP vector (pGFP::3′UTR_{CTA1}). For statistical analysis, ANOVA two-way test was performed using GraphPad Prism (version 7.0.0 for Windows, GraphPad Software, San Diego, California USA, www.graphpad.com). Error bars represent the standard deviation (SD). $P < 0.05$ was considered statistically significant.

2.12. qPCR expression analysis

A quantitative transcript analysis (qPCR) was performed to determine the expression levels of *ScSUM1* and *LkSUM1* and the adhesin encoding genes *AED1*, *EPA1*, *EPA6*, *EPA20* and *EPA22*. Cells were grown as described above. RNA was isolated using TRIzol Reagent (Invitrogen) according to the manufacturer's instructions. Extracted RNA was treated with recombinant DNase I, RNAse free (Roche Applied Science) and cDNA was synthesized with SuperScript II Reverse Transcriptase (Invitrogen) using oligo (Dt) primer. qPCR was carried out using Fast SYBR Green Master Mix (Thermo Fisher Scientific) in PIKOREAL 96 Real-Time PCR System (Thermo Scientific). *ACT1* was used as housekeeping control for all three species: *C. glabrata*, *S. cerevisiae* and *L. kluyveri*. The reverse and forward oligonucleotides used for qPCR were designed using the PrimerQuest Tool from Integrated DNA Technologies, Inc. (https://www.idtdna.com/ Primerquest/Home/Index) (Table 3, *CgACT1* #1266-#1267, *ScACT1* #A16-#A17, *LkACT1* #H46-H47, *CgSUM1* #2750-#2751, *ScSUM1* #2764-#2765, *LkSUM1* #2770-#2771, *AED1* #2927-#2928, *EPA1* #2931-#2932, *EPA6* #2939-#2940, *EPA20* #2949-2950, *EPA22* #2955-2956). The threshold cycle ($2^{-\Delta Ct}$) method was used to calculate the differences in gene expression (Asp, 2018; Haring et al., 2007; Lacazette, 2017). Statistical analysis (Mann Whitney test) was performed using GraphPad Prism (version 7.0.0 for Windows, GraphPad Software, San Diego, California USA, www.graphpad.com).

2.13. Codon usage analysis

A codon usage analysis was made between *C. glabrata*, *S. cerevisiae* and *L. kluyveri*. The Codon Usage Database (https://www.kazusa.or.jp/codon/) and the Graphical Codon Usage Analyzer (http://gcua.schoedl.de/index.html, Fuhrmann et al., 2004) were used to make the comparisons.

2.14. Neutrophil survival assay

Neutrophil Survival Assay was done as described previously (Gutiérrez-Escobedo et al., 2020) with the following modification. The

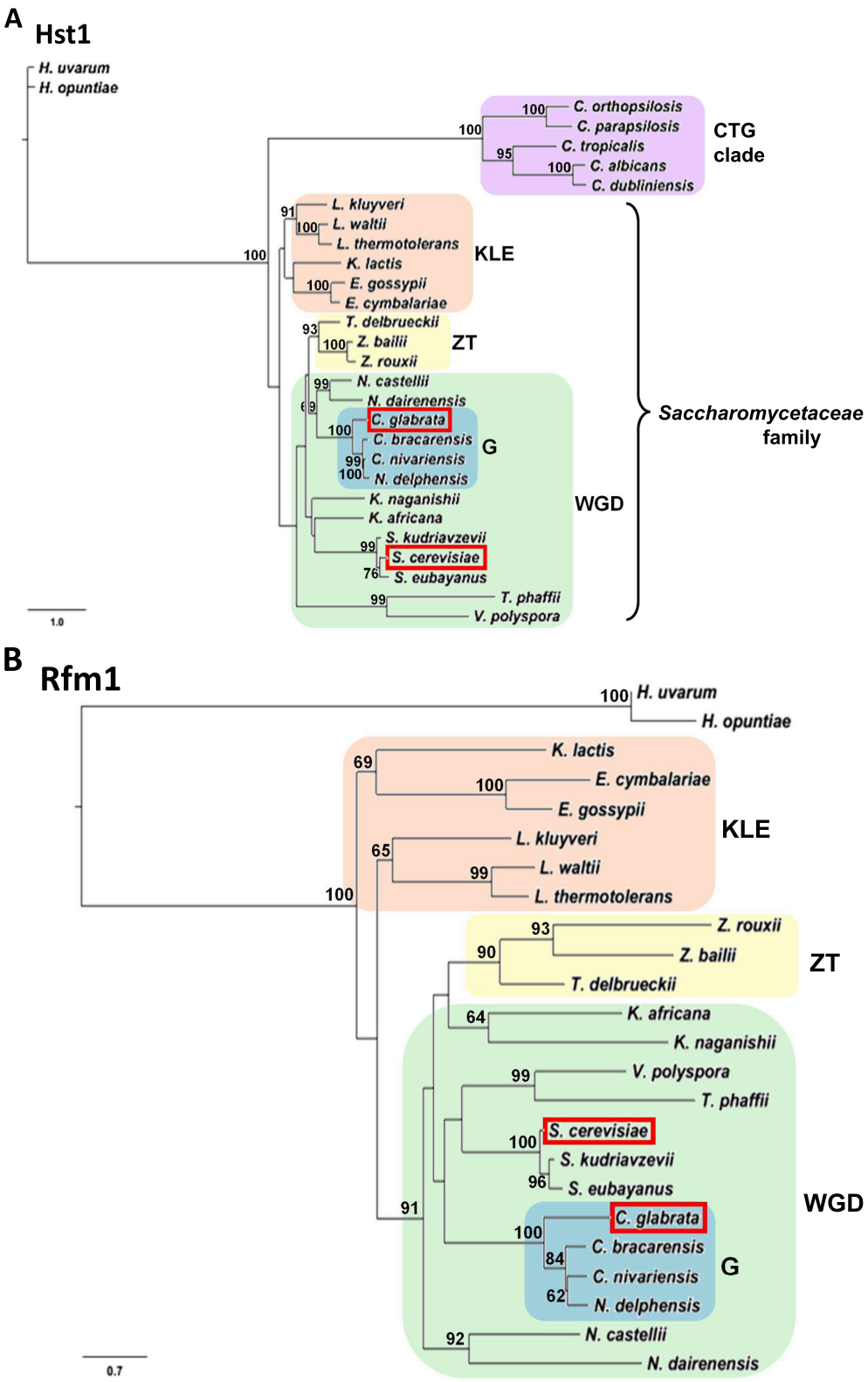

Fig. 1. Phylogenetic analysis of Hst1, Sum1 and Rfm1. Phylogenetic analysis of Hst1 (A), Rfm1 (B) and Sum1 (C). CTG clade, species that changed the CTG codon usage to serine (*Debaryomycetaceae* family); KLE, *Kluyveromyces-LachanceaEremothecium* clade; ZT, *Zygosaccharomyces-Torulaspora* clade; WGD, whole genome duplication clade; G, *Nakaseomyces/Candida* clade (*glabrata* group). KLE, ZT, WGD, and G belongs to *Saccharomycetaceae* family. The percentage of the replicates in which the associated taxa clustered together are shown next to the branches. See Materials and Methods 2.8.

preparation of yeast cells as well as the obtaining of neutrophils was carried out as indicated in the reference. For the Neutrophil Survival Assays, neutrophils were added into 96 well plates together with yeast cells (2x105) at a MOI 1:1. Yeast cells were also added to wells without neutrophils, as input. 96 well plates were incubated for 3 h at 37°C and CO_2 5% (instead of 2 h as indicated in Gutiérrez-Escobedo et al., 2020). Neutrophils were lysed after incubation, and the cell suspension of recovered *C. glabrata* cells was diluted, plated onto YPD plates, and incubated for 48 h at 30°C. CFU were determined and the survival percentage was scored. For statistical analysis, ANOVA one-way test was performed using GraphPad Prism.

C Sum1

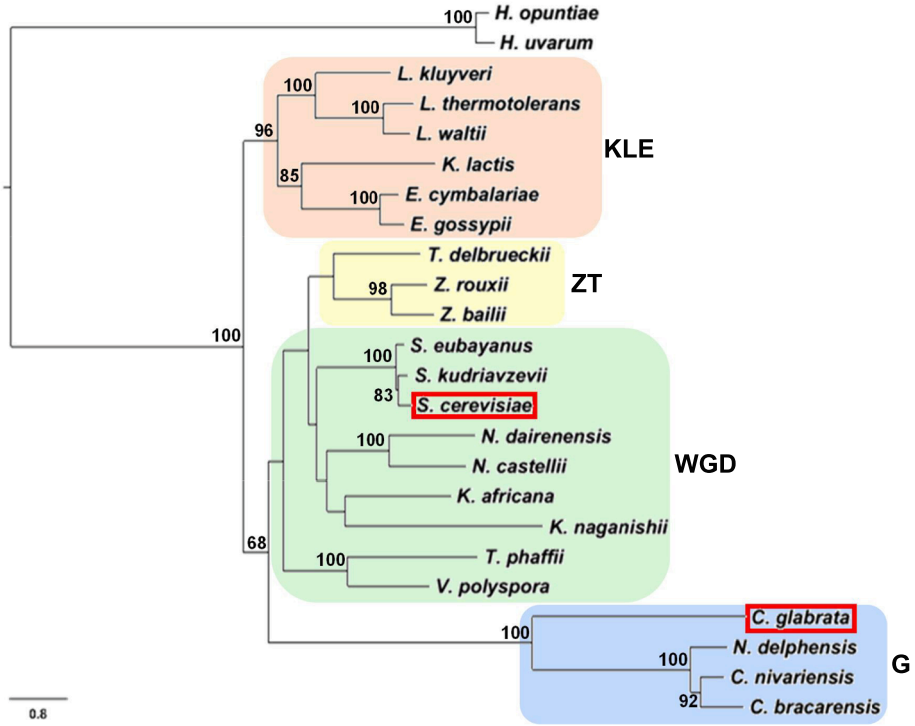

Fig. 1. (*continued*).

2.15. Adherence to HeLa cells assay

HeLa cells were grown, fixed and *C. glabrata* adherence was done as described (Leiva-Peláez et al., 2018; Martínez-Jiménez et al., 2013). *C. glabrata* cells were grown in YPD for 48 h at 30°C and OD_{600nm} adjusted to 0.5 in Hanks Balanced Salt Solution with $CaCl_2$ (5 Mm). Yeast cells were added to fixed HeLa cells in a 24-well plate and incubated for 3 h at room temperature. Plates were washed 4 times with HBSS with $CaCl_2$. Adhered *C. glabrata* cells were recovered by scraping the wells. Serial dilutions were made in distilled water, plated onto YPD plates, and incubated at 30°C for 48 h. CFUs were scored and percentage adherence was calculated. For statistical analysis, ANOVA with Dunnetts multiple test was performed using GraphPad Prism. Error bars represent the standard deviation (SD). (*** $P < 0.0001$, ** $P < 0.01$, * $P < 0.05$).

2.16. Chromatin immunoprecipitation assay (ChIP)

The ChIP assay was performed as previously described (López-Fuentes et al., 2018). *C. glabrata* cells were grown in 10 ml of minimal medium during 48 h. at 30°C. Cultures were adjusted to an OD_{600nm} of 1 in a total volume of 150 ml of distilled water. The antibodies used were α-*FLAG* and α-*cMyc* (SIGMA-ALDRICH, Co.). Immunoprecipitated DNA and input DNA were used as a template for Qpcr reactions. Qpcr was carried out using Fast SYBR Green Master Mix (Thermo Fisher Scientific) in PIKOREAL 96 Real-Time PCR System (Thermo Scientific). Primers used are indicated in Fig. 4C, E, and S3 and are described in Table 3. Percentage enrichment relative to the untagged BG14 strain was calculated. The percent enrichment of input was calculated by percent input method, with the equation 100*2^-(Adjusted Cq Input DNA – Cq immunoprecipitated DNA). Data plotted are mean values ± SD. Statistical analysis was performed with GraphPad Prism (version 7.0.0 for Windows, GraphPad Software, San Diego, California USA, www.graphpad.com) through a two-tailed unpaired Student's *t* test.

3. Results and discussion

3.1. Phylogeny of the HRS complex

C. glabrata and *S. cerevisiae* are closely related phylogenetically, however, there are clear genetic differences between these two fungal species (Gabaldón et al., 2013). The Hst1-Rfm1-Sum1 complex (HRS-C) controls the expression of different genes in both species. While *Sc*HRS-C controls the mid-sporulation genes, the *Cg*HRS-C also controls the oxidative stress response, multidrug resistance and genes encoding the high affinity niacin transporters (Domergue et al., 2005; Ma et al., 2009; Orta-Zavalza et al., 2013; Piekarska et al., 2010) Here, we decided to determine the phylogenetic relationship and the evolutionary divergence of the proteins of the *Cg*HRS-C. We made a phylogenetic analysis based on the *C. glabrata* phylum (Gabaldón et al., 2013) (See Materials and Methods 2.8). Our analysis of Hst1 in several species of the *Saccharomycetaceae* family indicates that it is present in all these species. However, it evolved differently in the species that conserved the use of the CUG codon (leucine) like *S. cerevisiae*, *C. glabrata*, *Lachancea kluyveri* than in the species that changed the CUG codon for serine like *Candida albicans* (Fig. 1A). Analysis of Rfm1 and Sum1 shows that these proteins are absent in the CTG clade (Fig. 1B and C). The analysis of Rfm1 indicates that it is conserved within the *Saccharomycetaceae* family. For Sum1, the analysis shows a distant phylogenetic relation between the *glabrata* group and the other members of the *Saccharomycetaceae* family (Fig. 1C). These results are consistent with the ORFs' shared similarity / identity and are syntenic between *C. glabrata* and *S. cerevisiae*: *Sc*Hst1 and *Cg*Hst1 are 61.3% identical (72.9% similar), *Sc*Rfm1 and *Cg*Rfm1 are 35.3% identical (55.8% similar) and *Sc*Sum1 and *Cg*Sum1 are 11% identical (22.4% similar) across the entire length of the proteins. This bioinformatic analysis is consistent with the description of *Sc*Sum1 controlling the expression of MMG, whereas *C. glabrata* has no mating cycle or meiosis. Instead, *Cg*Sum1 controls the expression of other genes required for resistance to xenobiotics, oxidative stress, and adherence

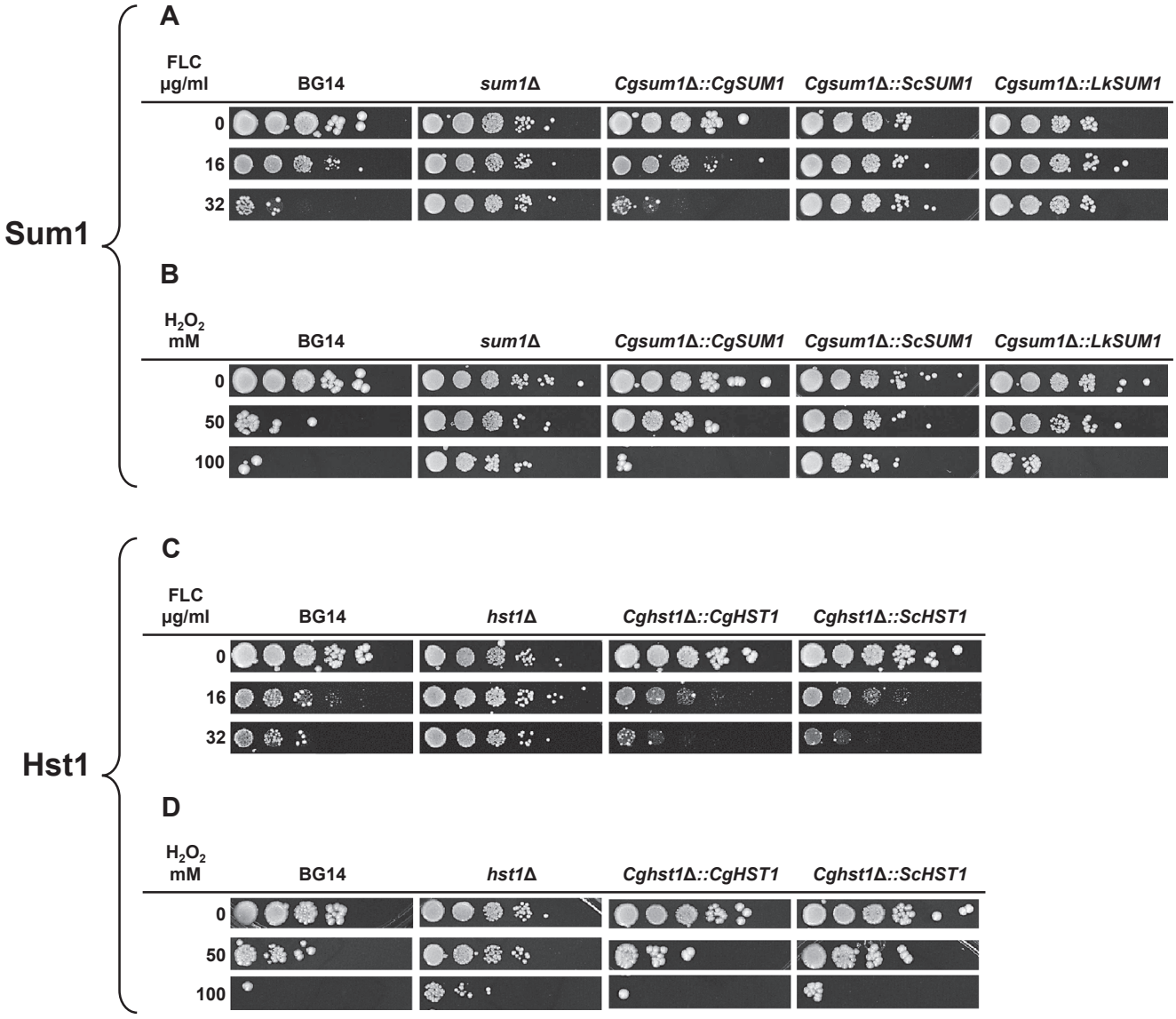

Fig. 2. Heterologous complementation of *HST1* and *SUM1*. *C. glabrata sum*1Δ and *hst*1Δ mutant strains were transformed with *CgSUM1*, *ScSUM1* and *LkSUM1* and *CgHST1* and *ScHST1* respectively and screened for functional complementation. *C. glabrata* parental strain (BG14), *sum*1Δ (CGM1232), *Cgsum*1Δ::*CgSUM1* (CGM1611), *Cg*sum1Δ::*ScSUM1* (CGM3192), *Cg*sum1Δ::*LkSUM1* (CGM3148), *hst*1Δ (CGM84), *Cghst*1Δ::*CgHST1* (CGM1605) and *Cghst*1 Δ::*ScHST1* (CGM3935) were grown for 48 h in YPD at 30°C. For the fluconazole (FLC) complementation phenotype, OD_{600nm} were adjusted to 0.5 and serial dilutions were prepared and spotted on plates containing 16 µg/ml and 32 µg/ml of FLC (A and C). For H_2O_2 complementation phenotype, cells were diluted in YPD and after 7 doublings cells were exposed to 50 mM and 100 mM of H_2O_2. After 3 h, cells were washed and plated onto YPD plates (B and D). Plates were incubated at 30°C for 48 h. Experiments were done at least three times. See Materials and Methods 2.9 and 2.10 and Table 1.

(Domergue et al., 2005; Ma et al., 2009; Orta-Zavalza et al., 2013; Piekarska et al., 2010).

3.2. Functional conservation of Hst1 and Sum1

The phylogenetic analysis of the HRS-C showed that the HRS evolved differently within the *glabrata* group and that the individual members of the complex evolved differently. Sum1, the DNA binding protein, is the most distantly related phylogenetically compared to Rfm1 and Hst1 within the species post-WGD. Based on the phylogenetic analysis, we decided to show if there is functional conservation of *Sc*Sum1, *Lk*Sum1 and *Sc*Hst1 in *C. glabrata* (*Lachancea kluyveri* (*Lk*) diverged from *S. cerevisiae* and *C. glabrata* before the whole genome duplication). For the heterologous complementation assay, we PCR fused the *ScHST1* ORF, *LkSUM1* ORF, and *ScSUM1* ORF with their respective *C. glabrata* cognate promoter and 3′UTR regions. These plasmids were integrated in the *Cghst*1Δ(*hst*1Δ::P_{CgHST1}::*ScHST1*::3′UTR_{CgHST1}) and *Cgsum*1Δ (*sum*1Δ::P_{CgSUM1}::*ScSUM1*::3′UTR_{CgSUM1} and *sum*1Δ::P_{CgSUM1}::*LkSUM1*::3′UTR_{CgSUM1}) loci to replace the corresponding *C. glabrata* ORFs. Positive controls were the reconstituted strains *Cghst*1Δ (*hst*1Δ::P_{CgHST1}::*CgHST1*::3′UTR_{CgHST1}) and *Cgsum*1Δ (*sum*1Δ::P_{CgSUM1}::*CgSUM1*::3′UTR_{CgSUM1}) with *CgHST1* and *CgSUM1*, respectively. *Cghst*1Δ and *Cgsum*1Δ strains have a slow grow phenotype and are less susceptible to FLC and H_2O_2. Cells were grown and exposed to FLC and H_2O_2 as described in the legend to Fig. 2.

3.2.1. Sum1

BG14 parental strain is sensitive and *sum*1Δ is resistant to 32 µg/ml of FLC (Fig. 2A). *sum*1Δ complemented with *CgSUM1* becomes sensitive to 32 µg/ml of FLC, however *sum*1Δ::*ScSUM1* and *sum*1Δ::*LkSUM1* remained resistant to 32 µg/ml of FLC. The same results are observed for the H_2O_2 assay. BG14 is sensitive and *sum*1Δ is resistant to 100 mM of

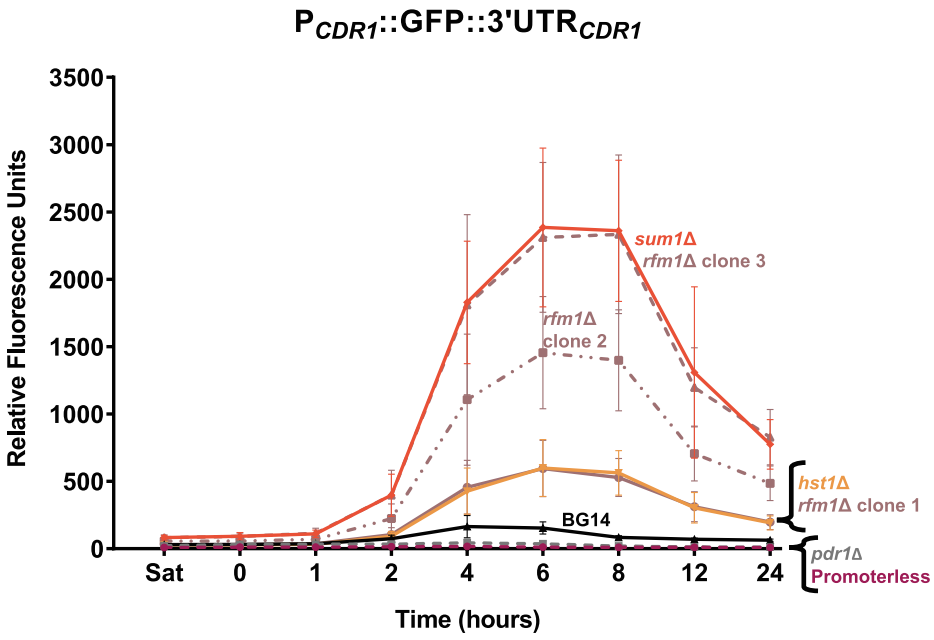

Fig. 3. Hst1, Rmf1 and Sum1 regulation of *CDR1* expression. Strains BG14 (CGM3756), *hst*1Δ (CGM3758), *sum*1Δ (CGM3760), *rfm*1Δ (CGM1234), and *pdr*1Δ (CGM3778) each carrying plasmid pP$_{CDR1}$::GFP::3′UTR::$_{CDR1}$ [pVF65] integrated in the *CDR1* locus and CGM514 (BG14 p::GFP::3′UTR$_{HIS3}$ promoterless vector [pMC14]) were grown for 48 h at 30°C in SC-Ura media and diluted into fresh media. Samples were taken every 2 h. Yeast cells were washed and resuspended in 1 ml sterile water and fluorescence was determined by flow cytometry analysis using a FACSCalibur flow cytometer (BD Biosciences). Experiments were repeated at least three times in triplicate. For statistical analysis, ANOVA two-way test was performed using GraphPad Prism. Error bars represent the standard deviation (SD) of at least three biological replicates with two technical replicates each. $p < 0.05$ was considered statistically significant. See Materials and Methods 2.11 and Tables 1 and 2.

H_2O_2 (Fig. 2B). *sum*1Δ complemented with *CgSUM1* becomes sensitive to 100 mM of H_2O_2, however *sum*1Δ::*ScSUM1* and *sum*1Δ::*LkSUM1* did not become sensitive to 100 mM of H_2O_2 (Fig. 2B).

3.2.2. *Hst1*

BG14 is sensitive and *hst*1Δ is resistant to 32 μg/ml of FLC (Fig. 2C) and *hst*1Δ grows slower than BG14 (see 0 μg/ml of FLC, Fig. 2C). *hst*1Δ strains complemented with both *CgHST1* and *ScHST1* become sensitive to 32 μg/ml of FLC (Fig. 2C) and grow faster than *hst*1Δ strain (see 0 μg/ml of FLC Fig. 2C). For the H_2O_2 assay, BG14 is sensitive and *hst*1Δ is resistant to 100 mM of H_2O_2 with the slow growing phenotype (see 0 mM H_2O_2 Fig. 2D). *hst*1Δ strains complemented with *CgHST1* and *ScHST1* become sensitive to 100 mM of H_2O_2 and the slow growth phenotype is complemented as well (Fig. 2). These functional heterologous complementation assays are consistent with the phylogenetic evolutionary analysis of Hst1 and Sum1. To show that the absence of complementation of *ScSUM1* and *LkSUM1* genes in *C. glabrata* is not due to lack of expression of the heterologous genes, we made a quantitative analysis of the transcripts (qPCR) and showed that *ScSUM1* and *LkSUM1* genes are being expressed (Fig. S1). In addition, we made a codon usage comparison between *C. glabrata*, *S. cerevisiae* and *L. kluyveri* (Codon Usage Database (https://www.kazusa.or.jp/codon/) and the Graphical Codon Usage Analyzer (http://gcua.schoedl.de/index.html)). The differences in codon usage based on relative adaptiveness are 5.5% between *C. glabrata* and *S. cerevisiae* and 12.98% between *C. glabrata* and *L. kluyveri*. (Fig. S2), indicating that the lack of *Sc*Sum1 and *Lk*Sum1 complementation is not due to a different use of codons between species. These data suggest that the *Cg*HRS-C diverged phylogenetically to control the expression of stress response genes.

Taken together the bioinformatic analysis and the functional complementation assays, they indicate that in spite of the phylogenetic relationship between non-pathogenic *S. cerevisiae* and opportunistic pathogen *C. glabrata*, the global regulation of many genes and the activity of specific proteins diverged in *C. glabrata* to become a successful pathogen. For example, a) the *Cg*HRS-C controls the expression of the oxidative stress response, adherence and xenobiotic resistance (Orta-Zavalza et al., 2013), while *Sc*HRS-C controls the expression of mid-sporulation genes (Piekarska et al., 2010), b) *C. glabrata* has subtelomeric genes (*EPA*) that encode cell wall proteins that mediate adherence to host epithelial cells and biofilm formation, in contrast the *S. cerevisiae FLO* genes some of which are subtelomeric, encode for cell wall proteins that mediate flocculation between yeast cells but not adherence to epithelial cells or biofilm formation (Castaño et al., 2006), c) The transcription factor *Sc*Pdr1, which controls the expression of ABC transporters and is constitutively expressed, has a paralogue, Pdr3. As opposed to Pdr1, Pdr3 is autoregulated and is activated in ρ^0 cells (petite cells with no mitochondrial DNA) (Hallstrom and Moye-Rowley, 2000). Interestingly, there is only one *Cg*Pdr1 but with the activity of both *Sc*Pdr1 and *Sc*Pdr3 (Delaveau et al., 1994; Moye-Rowley, 2019).

3.3. *Sum1 and Rfm1 are negative regulators of CDR1 expression*

In a previous work, we obtained genetic and biochemical evidence that Hst1 modulates the multidrug and the oxidative stress resistance in *C. glabrata* by controlling the expression of *PDR1*, *CDR1*, *MSN4* and *CTA1* (Orta-Zavalza et al., 2013). Furthermore, we showed that Sum1 and Rfm1 behave like Hst1: the absence of Sum1 confers resistance to H_2O_2 and FLC (Fig. 2 and Orta-Zavalza et al., 2013). In *S. cerevisiae*, it has been proposed that Sum1 binds to promoters of mid-sporulation genes (MSG) and recruits Hst1 through Rfm1 as a connector protein, thus repressing their expression (Pak and Segall, 2002; Piekarska et al., 2010). It has also been proposed that this negative regulation occurs through the competition for the binding sites (YGNCACAAAA) between Sum1 and Ndt80 (activator of MSG), where Sum1 prevents the binding of Ndt80 (Pierce et al., 2003). Given that it is not known whether the repression mechanism of the *Cg*HRS-C is similar to that in *S. cerevisiae*, we decided to analyze *CDR1* regulation in the absence of Hst1, Sum1 and Rfm1. We cloned in an integrative plasmid a transcriptional fusion between *CDR1* promoter and GFP (pP$_{CDR1}$::GFP::3′UTR$_{CDR1}$) and integrated this plasmid in its genomic locus in the parental strain BG14 and into the single mutant strains *hst*1Δ, *sum*1Δ, *rfm*1Δ and *pdr*1Δ. The negative control was BG14 carrying a promoterless GFP plasmid. The promoter activity was measured by flow cytometry analysis (see legend to Fig. 3 and Materials and Methods 2.11) in stationary and log phase cultures. *CDR1* expression is slightly increased at 4 h. of growth in the BG14 strain (Fig. 3). In contrast and consistent with our genetic data, *CDR1* expression is 3-fold higher in the *hst*1Δ strain and ten-fold higher in the *sum*1Δ strain compared with BG14 (Fig. 3). *CDR1* expression is dependent on Pdr1 since *CDR1* expression is abrogated in the *pdr*1Δ mutant strain (Fig. 3) (Ferrari et al., 2009; Morschhäuser, 2010; Paul and Moye-Rowley, 2014).

It should be noted that we always test several independently isolated

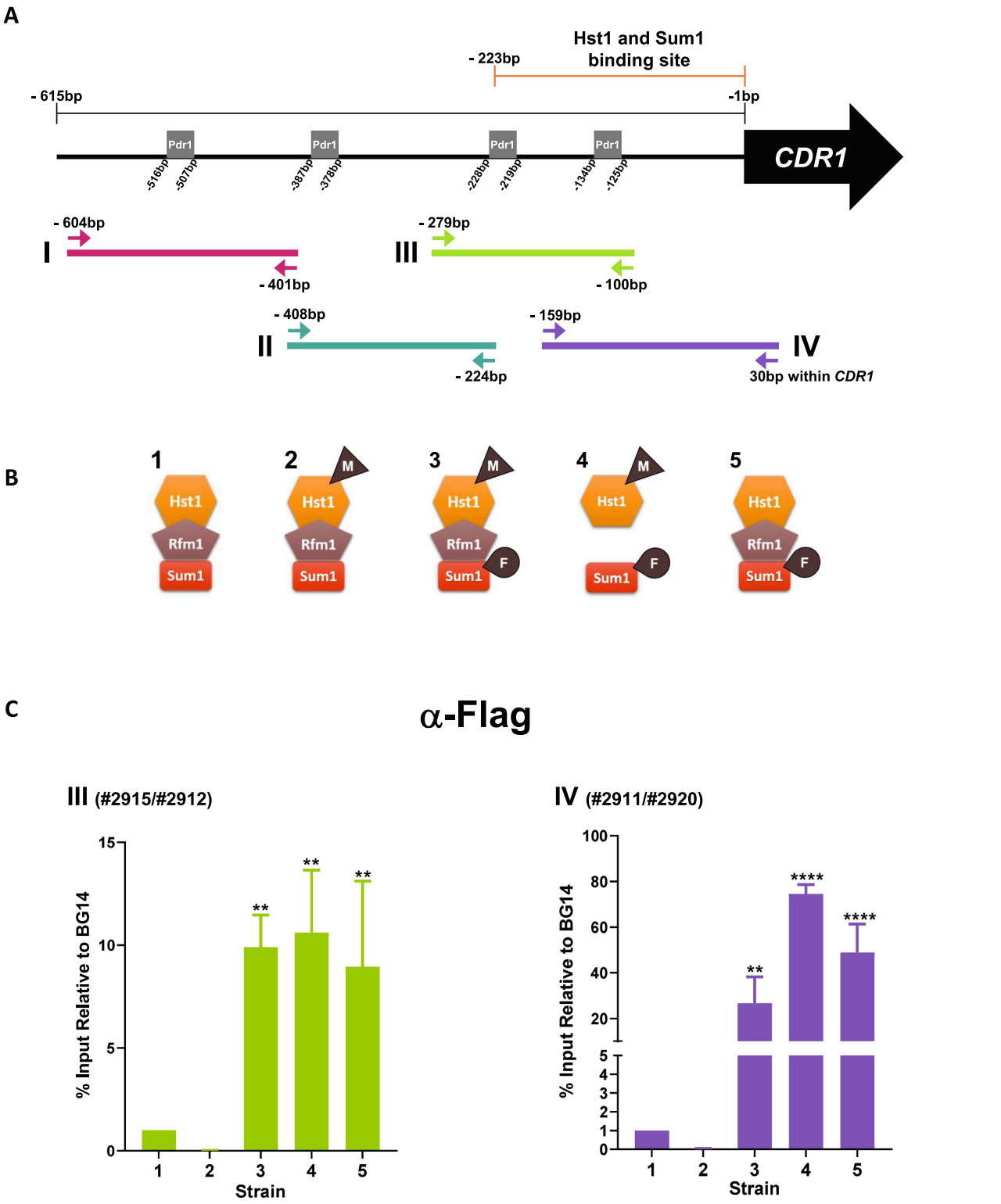

Fig. 4. Binding profile of Hst1 and Sum1 in the *CDR1* upstream sequence. (A) Map of the *CDR1* upstream sequence (615 bp) for the ChIP assay. Schematic representation for *CDR1* gene is not to scale. Amplified fragments (Roman numerals I to IV) are shown and represented with a color bar; arrows with numbers indicate the position of the primer pairs for qPCR. Pdr1 binding sites are indicated. (B and D) Schematic representation of the untagged and tagged HRS complexes. (C) ChIP assay using α-*FLAG* and (E) ChIP assay using α-*cMyc*. Enrichment of each of the four fragments is represented as percentage of the input relative to BG14 enrichment. Each graph (I - IV) corresponds to one of the four amplified fragments and are color coded in the schematic map (A). Amplified fragments I and II are in shown in Figure S3. Numbers in parentheses identify the primer pairs used for each fragment (Table 3). Each bar (1 to 5) corresponds to each of the strains used in the assay (B and D). ChIP samples were obtained as previously described in Material and Methods (2.16). Values are mean (±SD) of three biological replicates each of them with three technical replicates and represent the percentage of the input relative to BG14 enrichment. Standard deviation (SD) is shown by error bars. * $P < 0.05$, ** $P < 0.01$, *** $P < 0.001$, *** $P < 0.0001$. (B and D) Strains used (1) BG14, (2) Hst1-*cMyc* (CGM934), (3) Hst1-*cMyc* Sum1-*FLAG* (CGM982), (4) Hst1-*cMyc* Sum1-*FLAG* *rfm*1Δ (CGM1294), and (5) Sum1-*FLAG* (CGM1340). Proteins tagged at the C-terminal end.

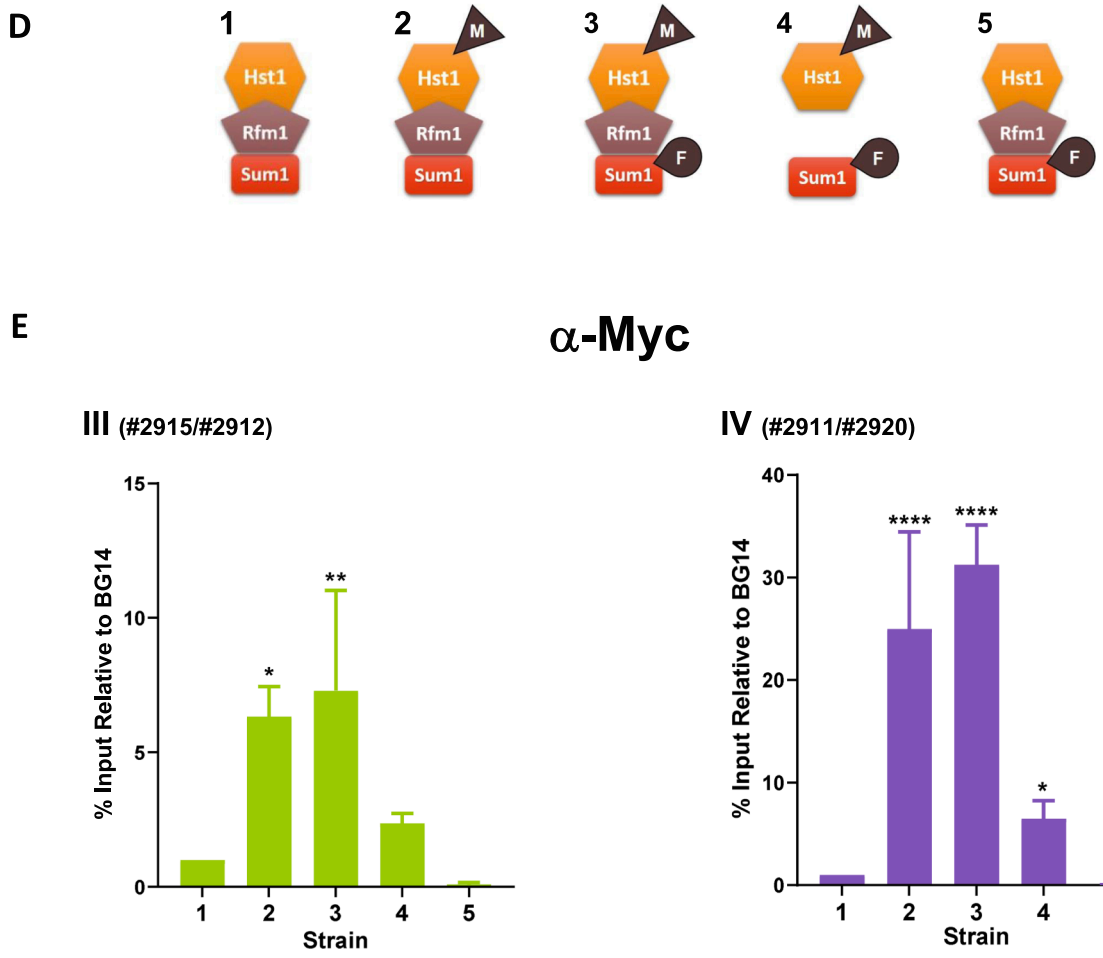

Fig. 4. (*continued*).

colonies of our mutants, and we found that *CDR1* expression in three independent *rfm*1Δ clones display different phenotypes: clone 1 behaves like *sum*1Δ, clone 2 behaves like *hst*1Δ and clone 3 shows an intermediate phenotype (Fig. 3, see section 3.4). These data indicate that all three proteins, Sum1, Hst1 and Rfm1 are required for full repression of *CDR1* expression, that Sum1 can bind to DNA independently of Hst1 and Rfm1 and that Hst1 requires both the presence of Sum1 and Rfm1 to fully function as a negative regulator. It is clear Rfm1 is required for the integrity of the HRS-C (see section 3.4 and Orta-Zavalza et al., 2013), but how Rfm1 modulates Sum1 activity is still unknown.

3.4. Sum1 and Rfm1 bind to the CDR1 promoter

To further understand how the HRS-C regulates *CDR1* expression, we determined the binding profiles of Sum1 and Hst1 in the *CDR1* promoter and how the absence of Rfm1 could affect their binding. We performed ChIP-qPCR assays with *C. glabrata* tagged strains (Fig. 4B and D): *Hst1-cMyc* (CGM934), *HST1-cMyc SUM1-FLAG* (CGM982), *HST1-cMyc SUM1-FLAG rfm*1Δ (CGM1294), *SUM1-FLAG* (CGM1340), and BG14 (untagged) as negative control strain (Table 1, legend to Fig. 4 and Materials and Methods 2.16). We analyzed a 615 bp region upstream from the ATG of *CDR1* with 4 pairs of primers (Fig. 4A sections I, II, III and IV). The analysis with both antibodies, α-*FLAG* and α -*cMyc*, shows that Hst1 and Sum1 are not present in sections I and II (Supplementary Fig. S3C and S3D). However, Hst1 and Sum1 are bound in sections III and IV and in particularly, Hst1 and Sum1 are highly enriched in section IV (Fig. 4C and E). Given that there is no binding in regions I and II and there is an overlap between regions II and III, the binding of the HRS-C must be between −1bp and −223 bp upstream of the ATG of *CDR1* (Fig. 4A).

The absence of Rfm1 has different effects in the binding of Sum1 and Hst1. In the *rfm*1Δ, the binding profile of Hst1 is severely reduced in both sections III and IV, but some Hst1 can still be detected (Fig. 4E columns 4). Conversely, in the absence of Rfm1, Sum1 binding in sections III and IV is not affected (Fig. 4C columns 4). There is higher enrichment for Sum1 with α-FLAG (Fig. 4C-IV) compared to Hst1 with α-*cMyc* (Fig. 4E-IV). This could be due to differences in antibody recognition of the tagged proteins. These results show that: a) the HRS-C binds to the *CDR1* promoter, b) Hst1 binding depends on Rfm1 and c) Sum1 binds independently of Rfm1 and Hst1.

The genetic and the biochemical data from the analysis of the *sum*1Δ, *hst*1Δ and *rfm*1Δ is consistent with the binding profile of these proteins (Orta-Zavalza et al., 2013), however is it still unclear how *rfm*1Δ affects the expression of *CDR1* (Fig. 3). The expression of *CDR1* in clone 1 (*rfm*1Δ) and clone 2 (*rfm*1Δ) can be explained due to the reduced presence of Hst1 (Figs. 3 and 4E). Interestingly, clone 1 (*rfm*1Δ) expresses *CDR1* to the same extent as the *sum*1Δ; even though Sum1 is still present at the *CDR1* promoter, however no DNA-binding domain has been identified in Sum1 (Conserved Domain Database, National Center for Biotechnology Information, U.S. National Library of Medicine, https://www.ncbi.nlm.nih.gov/cdd). These data suggest the presence of additional proteins in the HRS-C that could be modulating the DNA binding activity of the HRS-C.

The binding of Hst1 and Sum1 in this region is consistent with the presence of two Pdr1 recognition sites (−228 TTCCACGGGA −219 and −134 CTCCACGGGA −125) (Fig. 4A) (Sanglard et al., 1999). Hst1 creates a local silent chromatin which prevents Pdr1 binding, thus resulting in lack of *CDR1* expression. The fact that *CDR1* is overexpressed in the absence of any inducer in the *sum*1 Δ or *hst*1Δ

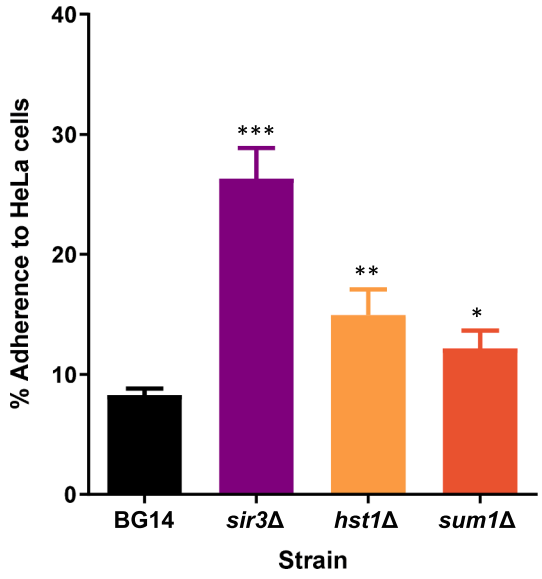

Fig. 5. *hst*1Δ and *sum*1Δ adherence to HeLa cells. *C. glabrata* BG14, *sir*3Δ (BG676) as positive control, *hst*1Δ (CGM84) and *sum*1Δ (CGM1232) were grown in YPD medium for 48 h at 30°C and OD_{600nm} adjusted to 0.5. Yeast cells were added to fixed HeLa cells in 24-well plates and incubated for 3 h at room temperature. Cells were recovered by scraping the wells and serial dilutions were made in distilled water, plated onto YPD plates, and incubated at 30°C for 48 h. Each of the three biological replicates was made with triplicate technical replicates. For statistical analysis, ANOVA with Dunnetts multiple test was performed using GraphPad Prism (version 7.0.0 for Windows, GraphPad Software, San Diego, California USA, www.graphpad.com). Error bars represent the standard deviation (SD). (, * $P < 0.05$, ** $P < 0.01$, *** $P < 0.001$). All mutant strains are significantly different from parental strain BG14 that is considered non-adherent under the growth condition tested. Less than 10% non-adherent, 10 %20% slightly adherent and 20–45% hyper-adherent. See Materials and Methods 2.15.

backgrounds suggests that Pdr1 expression (which controls its own expression) could be increased as well. Pdr1 activity is tightly regulated because overexpression of Pdr1 is toxic to the cell in *S. cerevisiae*. Both, *hst*1Δ, *sum*1Δ and *rfm*1Δ strains show slow growth phenotype (this work and Borah et al., 2014; Noble et al., 2013; Orta-Zavalza et al., 2013; Paul et al., 2018; Whaley et al., 2018). Increased levels of Pdr1 could titrate the negative regulators and lead to increased Pdr1-dependent gene expression (Khakhina et al., 2018; Tsai et al., 2006) or the negative regulation exerted by the HRS-C on *CDR1* expression could be overridden just by the increased levels of Pdr1. Alternatively, a member of the HRS-C could be a target for protein modification. Such is the case of *Sc*Sum1. *Sc*Sum1 represses transcription of *NDT80* which encodes a meiotic transcriptional activator. *Sc*Sum1is inactivated by phosphorylation allowing transcription of *NDT80*, thus inducing the cells to enter meiosis (Corbi et al., 2014).

3.5. Hst1 and Sum1 are dispensable for survival in neutrophils

It has been shown that exposure of *C. glabrata* cells to human neutrophils induces the expression of about 500 genes, including stress response genes like *CTA1*, *SOD2* and *PDR1* (Fukuda et al., 2013). Given that HRS-C controls the expression of the oxidative stress response and regulates multidrug resistance, we then asked whether Hst1 and Sum1 play a role in *C. glabrata* interaction with human neutrophils. Human neutrophils were infected with parental strain BG14, *hst*1Δ and *sum*1Δ as described in the legend to Fig. S4. *hst*1Δ and *sum*1Δ mutant strains showed no defect in survival since both mutant strains show no significant difference with BG14 (Fig. S4). These results indicate that Hst1 and Sum1 are not required for survival in neutrophils. Since HRS-C negatively controls the expression of stress related genes, it could have been expected that the analysis of *hst*1Δ and *sum*1Δ in the presence of neutrophils could rather show an increase in survival. This is not the case given that *hst*1Δ and *sum*1Δ have a growth defect possibly due to overexpression of specific genes that together are toxic to the cell (possibly Pdr1, section 3.4). 23 genes in *C. glabrata* have been identified that are required for survival in the presence of neutrophils, however this group of genes are not HRS-C related genes (Seider et al., 2014).

3.6. Hst1 and Sum1 are required to prevent adherence to HeLa cells

C. glabrata has been shown to adhere to epithelial cells through the Epa adhesins (Castaño et al., 2005; Cormack et al., 1999). Many of the genes encoding the Epa adhesins are localized to the subtelomeric regions and their expression is controlled by chromatin-based subtelomeric silencing (Castaño et al., 2005; De Las Peñas et al., 2003). In addition to the subtelomeric silencing, there are other transcriptional regulators that control the expression of the *EPAs*. $Pdr1^{GOF}$ mutant induces the expression of the main adhesin Epa1 and the cells become hyper-adherent (Vale-Silva et al., 2013, 2016) and a microarray analysis with *hst*1Δ showed that Hst1 controls the expression of *EPA6*, *EPA20* and *EPA22* (Domergue et al., 2005; Ma et al., 2009). Here we asked if HRS-C could participate in controlling adherence of *C. glabrata* to cultured HeLa cells. Stationary cultures of BG14, *sir*3Δ, *hst*1Δ and *sum*1Δ were grown and added to fixed cultured HeLa cells (as described in the legend to Fig. 5 and Materials and Methods 2.15). Percentage of adherence is shown. Under these conditions, BG14 parental strain displays background levels of adherence (7%) while *sir*3Δ (Sir3 is a member of the Sir complex which is required for subtelomeric silencing) shows 28% adherence (Fig. 5). The *sir*3Δ mutant strain is hyper-adherent because many *EPA* genes are expressed due to the absence of subtelomeric silencing. *hst*1Δ and *sum*1Δ show a moderate percentage of adherence, 14%, and 13% to HeLa cells (Fig. 5). These results indicate that the HRS-C might be controlling the expression of a small set of *EPA* genes even in the presence of subtelomeric silencing. Subtelomeric silencing depends on the activity of NAD^+-dependent histone deacetylase, Sir2 (Castaño et al., 2003; De Las Peñas et al., 2003; Domergue et al., 2005). *EPA6*, *EPA20* and *EPA22* are additionally controlled by Hst1 (HRS-C), another NAD^+-dependent histone deacetylase (Castaño et al., 2005; Cormack et al., 1999; De Las Peñas et al., 2003; Domergue et al., 2005). Both Sir2 and Hst1 are inactivated if the levels of NAD^+ are reduced. Inactivation of these sirtuins induces the expression of *EPA* genes and the cells become hyper-adherent. It has also been reported that Aed1 (Awp5) protein, an adhesin that mediates adherence to endothelial cells (Desai et al., 2011) have been identified as one of the adhesins present into the *C. glabrata* cell wall, however its ligand is still unknown (de Groot et al., 2013, 2008; Kraneveld et al., 2011). In order to know if HRS-C controls the expression of adhesin encoding genes, we decided to evaluate the expression of *AED1*, *EPA1*, *EPA6*, *EPA20*, and *EPA22* by RT-qPCR, in *hst*1Δ, *rfm*1Δ, *sum*1Δ (HRS-C compromised), and *sir*3Δ and BG14 as control strains (Fig. 6). Results show that there is a significant increase in the expression of all the adhesins evaluated, except for *EPA20* (Fig. 6D). Interestingly, despite *AED1* being 1.8 kb from the telomere, its expression only increases in the absence of any of the HRS-C proteins, but not in the absence of Sir3 (Fig. 6A). *EPA1* expression is increased in the absence of the HRS-C to the same extent as in the *sir*3Δ strain (Fig. 6B). *EPA6* expression is increased in the absence of HRS-C but not as high as the increase in the *sir*3Δ, as has been previously shown (Domergue et al., 2005). Regulation of *EPA6* is mainly mediated by subtelomeric silencing, with a slight contribution of HRS-C (Fig. 6C). Contrary to *EPA6*, expression of *EPA22* which is located 14.1 kb from the telomere, is mediated mainly by the HRS-C with a slight contribution of subtelomeric silencing (Fig. 6E). The expression of *EPA20* is independent of subtelomeric silencing from the telomere (located at 25.8 kb from the telomere) and of HRS-C (Fig. 6D). These results suggest that HRS-C is an additional layer of transcriptional regulation for several subtelomeric adhesin encoding genes. Interestingly, HRS-C control the expression of

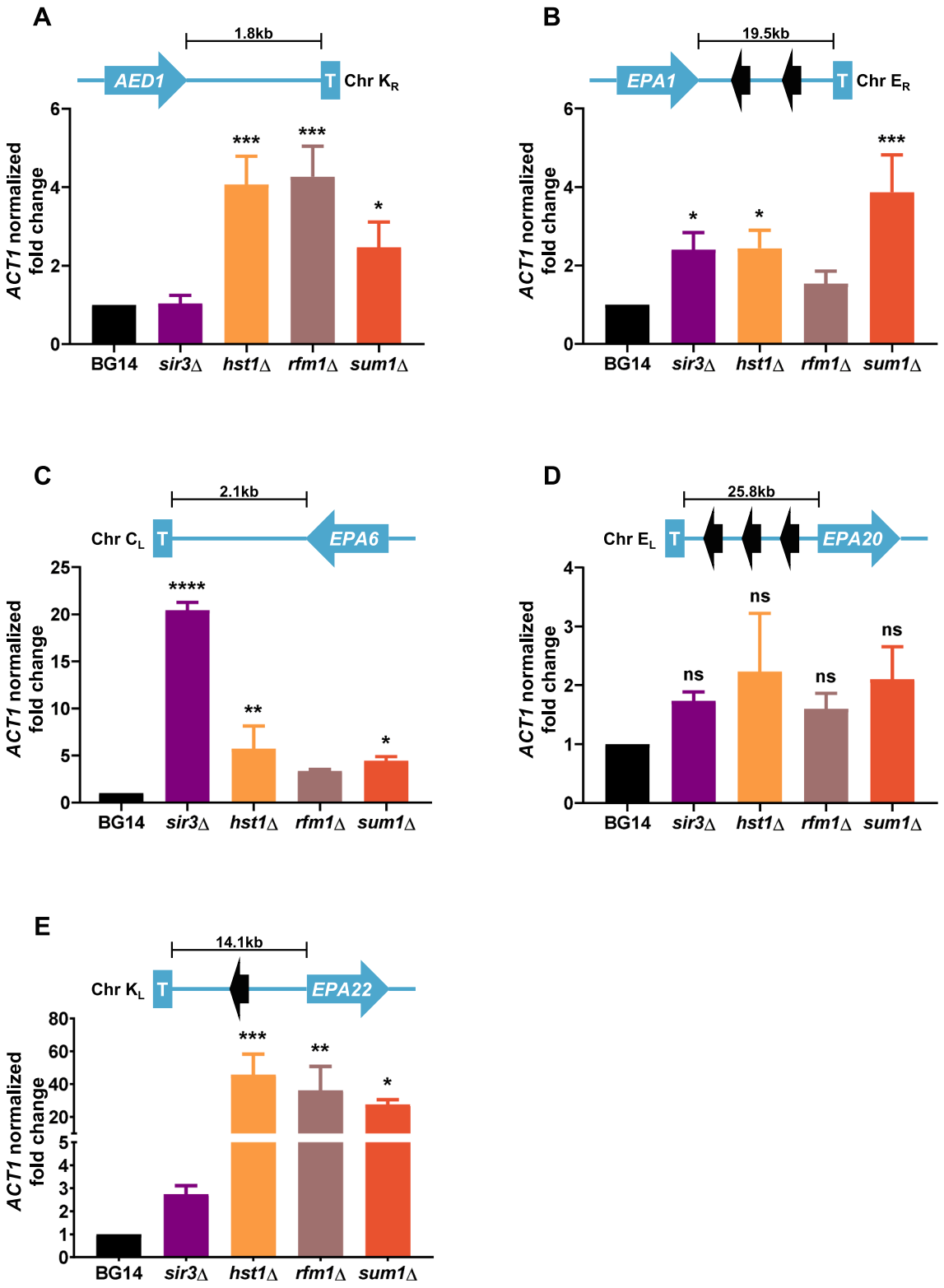

Fig. 6. Expression of *AED1*, *EPA1*, *EPA6*, *EPA20* and *EPA22*. Expression of (A) *AED1*, (B) *EPA1*, (C) *EPA6*, (D) *EPA20*, and (E) *EPA22* was analyzed by qPCR. RNA samples were isolated as previously described in Material and Methods (2.12). Values are mean (±SD) of three biological replicates with tree technical replicates and represent the relative expression of genes of interest. Data was normalized to 1.0 by *ACT1* expression levels. Standard deviation (SD) is shown by error bars. * $P < 0.05$, ** $P < 0.01$, *** $P < 0.001$, *** $P < 0.0001$, ns not significantly different.

AED1 independently of subtelomeric silencing despite its proximity to the telomere (1.8 kb).

Here, we showed that Sum1 in the HRS-C diverged functionally to control several stress-related genes implicated in virulence: adherence, resistance to xenobiotics and oxidative stress (Orta-Zavalza et al., 2013). It is possible that the HRS-C could be detecting environmental signals (directly or through signal transduction pathways) and modulate its transcriptional regulatory activity: binding to DNA for repression or

derepressing target genes. It is now important to identify which genes are regulated by HRS-C genome wide. Furthermore, it is likely that additional proteins are present in the HRS-C, which must be identified to fully understand the HRS-C activity.

CRediT authorship contribution statement

Norma Vázquez-Franco: Investigation, Software, Formal analysis, Writing – original draft. **Guadalupe Gutiérrez-Escobedo:** Investigation, Visualization, Writing – review & editing. **Alejandro Juárez-Reyes:** Writing – review & editing. **Emmanuel Orta-Zavalza:** Conceptualization, Methodology, Writing – review & editing. **Irene Castaño:** Conceptualization, Writing – review & editing. **Alejandro De Las Peñas:** Conceptualization, Formal analysis, Methodology, Project administration, Funding acquisition, Writing – review & editing.

Declaration of Competing Interest

The authors declare that they have no known competing financial interests or personal relationships that could have appeared to influence the work reported in this paper.

Acknowledgments

We thank Lina Riego Ruiz, Luis Fernando García Ortega and Cesaré Ovando Vázquez for technical assistance for the bioinformatic analysis. We thank Luis Salazar and Angélica Montoya for providing HeLa cells. This work was supported by an IPICYT and Consejo Nacional de Ciencia y Tecnología (CONACYT) fellowships to N.V.F. (225311). This work was supported by CONACYT grant no. A1-S-9550 to A.D.L.P.

Appendix A. Supplementary material

Supplementary data to this article can be found online at https://doi.org/10.1016/j.fgb.2021.103656.

References

Asp, P., 2018. How to combine ChIP with qPCR. Methods Mol. Biol. 1689, 29–42. https://doi.org/10.1007/978-1-4939-7380-4_3.

Ausubel, F.M., 1992. Short protocols in molecular biology. In: A Compendium of Methods From "Current Protocols in Molecular Biology," 2nd ed. John Wiley & Sons.

Baudin, A., Ozier-Kalogeropoulos, O., Denouel, A., Lacroute, F., Cullin, C., 1993. A simple and efficient method for direct gene deletion in Saccharomyces cerevisiae. Nucleic Acids Res. 21 (14), 3329–3330. https://doi.org/10.1093/nar/21.14.3329.

Borah, S., Shivarathri, R., Srivastava, V.K., Ferrari, S., Sanglard, D., Kaur, R., 2014. Pivotal Role for a Tail Subunit of the RNA Polymerase II Mediator Complex CgMed2 in Azole Tolerance and Adherence in Candida glabrata. Antimicrob. Agents Chemother. 58 (10), 5976–5986. https://doi.org/10.1128/AAC.02786-14.

Brachmann, C.B., et al., 1998. Designer deletion strains derived from Saccharomyces cerevisiae S288C: a useful set of strains and plasmids for PCR-mediated gene disruption and other applications. Yeast 14, 115–132. https://doi.org/10.1002/(SICI)1097-0061(19980130)14:2<115::AID-YEA204>3.0.CO;2-2.

Briones-Martin-del-Campo, M., Orta-Zavalza, E., Cañas-Villamar, I., Gutiérrez-Escobedo, G., Juárez-Cepeda, J., Robledo-Márquez, K., Arroyo-Helguera, O., Castaño, I., De Las Peñas, A., 2015. The superoxide dismutases of Candida glabrata protect against oxidative damage and are required for lysine biosynthesis, DNA integrity and chronological life survival. Microbiology 161, 300–310. https://doi.org/10.1099/mic.0.000006.

Byrne, K.P., Wolfe, K.H., 2005. The Yeast Gene Order Browser: Combining curated homology and syntenic context reveals gene fate in polyploid species 1456–1461. DOI: 10.1101/gr.3672305.

Castaño, I., Kaur, R., Pan, S., Cregg, R., Peñas, A.D.L., Guo, N., Biery, M.C., Craig, N.L., Cormack, B.P., 2003. Tn7-based genome-wide random insertional mutagenesis of Candida glabrata. Genome Res. 13 (5), 905–915. https://doi.org/10.1101/gr.848203.

Calvin, N.M., Hanawalt, P.C., 1988. High-efficiency transformation of bacterial cells by electroporation. J. Bacteriol. 170, 2796–2801. https://doi.org/10.1128/jb.170.6.2796-2801.1988.

Castaño, I., Cormack, B., De Las Peñas, A., 2006. Virulence of the opportunistic pathogen mushroom Candida glabrata. Rev. Latinoam. Microbiol. 48, 66–69.

Castaño, I., Pan, S.J., Zupancic, M., Hennequin, C., Dujon, B., Cormack, B.P., 2005. Telomere length control and transcriptional regulation of subtelomeric adhesins in Candida glabrata. Mol. Microbiol. 55, 1246–1258. https://doi.org/10.1111/j.1365-2958.2004.04465.x.

Corbi, D., Sunder, S., Weinreich, M., Skokotas, A., Johnson, E.S., Winter, E., 2014. Multisite phosphorylation of the Sum1 transcriptional repressor by S-phase kinases controls exit from meiotic prophase in yeast. Mol. Cell. Biol. 34 (12), 2249–2263. https://doi.org/10.1128/MCB.01413-13.

Cormack, B., Falkow, S., 1999. Efficient homologous and illegitimate recombination in the opportunistic yeast pathogen Candida glabrata. Genetics 151, 979–987. https://doi.org/10.1093/genetics/151.3.979.

Cormack, B.P., Ghori, N., Falkow, S., 1999. An adhesin of the yeast pathogen Candida glabrata mediating adherence to human epithelial cells. Science (80-.) 285 (5427), 578–582.

Cuéllar-Cruz, M., Briones-Martin-del-Campo, M., Cañas-Villamar, I., Montalvo-Arredondo, J., Riego-Ruiz, L., Castaño, I., De Las Peñas, A., 2008. High resistance to oxidative stress in the fungal pathogen *Candida glabrata* is mediated by a single catalase, Cta1p, and is controlled by the transcription factors Yap1p, Skn7p, Msn2p, and Msn4p. Eukaryot. Cell 7 (5), 814–825. https://doi.org/10.1128/EC.00011-08.

de Groot, P.W.J., Bader, O., de Boer, A.D., Weig, M., Chauhan, N., 2013. Adhesins in human fungal pathogens: Glue with plenty of stick. Eukaryot. Cell 12 (4), 470–481. https://doi.org/10.1128/EC.00364-12.

de Groot, P.W.J., Kraneveld, E.A., Yin, Q.Y., Dekker, H.L., Groß, U., Crielaard, W., de Koster, C.G., Bader, O., Klis, F.M., Weig, M., 2008. The cell wall of the human pathogen Candida glabrata: Differential incorporation of novel adhesin-like wall proteins. Eukaryot. Cell 7 (11), 1951–1964. https://doi.org/10.1128/EC.00284-08.

De Las Peñas, A., Pan, S.-J., Castaño, I., Alder, J., Cregg, R., Cormack, B.P., 2003. Virulence-related surface glycoproteins in the yeast pathogen Candida glabrata are encoded in subtelomeric clusters and subject to RAP1- and SIR-dependent transcriptional silencing. Genes Dev. 17 (18), 2245–2258. https://doi.org/10.1101/gad.1121003.

Delaveau, T., Delahodde, A., Carvajal, E., Subik, J., Jacq, C., 1994. PDR3, a new yeast regulatory gene, is homologous toPDR1 and controls the multidrug resistance phenomenon. Mol. Gen. Genet. MGG 244 (5), 501–511. https://doi.org/10.1007/BF00583901.

Desai, C., Mavrianos, J., Chauhan, N., 2011. Candida glabrata Pwp7p and Aed1p are required for adherence to human endothelial cells. FEMS Yeast Res. 11 (7), 595–601. https://doi.org/10.1111/j.1567-1364.2011.00743.x.

Domergue, R., Castaño, I., De Las Peñas, A., Zupancic, M., Lockatell, V., Hebel, J.R., Johnson, D., Cormack, B.P., 2005. Nicotinic acid limitation regulates silencing of Candida Adhesins during UTI. Science (80-.) 308 (5723), 866–870.

Edgar, R.C., 2004. MUSCLE: multiple sequence alignment with high accuracy and high throughput. Nucleic Acids Res. 32 (5), 1792–1797. https://doi.org/10.1093/nar/gkh340.

Ferrari, S., Ischer, F., Calabrese, D., Posteraro, B., Sanguinetti, M., Fadda, G., Rohde, B., Bauser, C., Bader, O., Sanglard, D., Filler, S.G., 2009. Gain of function mutations in CgPDR1 of Candida glabrata not only mediate antifungal resistance but also enhance virulence. PLoS Pathog. 5 (1), e1000268. https://doi.org/10.1371/journal.ppat.1000268.

Fuhrmann, M., Hausherr, A., Ferbitz, L., Schödl, T., Heitzer, M., Hegemann, P., 2004. Monitoring dynamic expression of nuclear genes in Chlamydomonas reinhardtii by using a synthetic luciferase reporter gene. Plant Mol. Biol. 55 (6), 869–881. https://doi.org/10.1007/s11103-004-2150-6.

Fukuda, Y., Tsai, H.-F., Myers, T.G., Bennett, J.E., Deepe, G.S., 2013. Transcriptional profiling of Candida glabrata during phagocytosis by neutrophils and in the infected mouse spleen. Infect. Immun. 81 (4), 1325–1333. https://doi.org/10.1128/IAI.00851-12.

Gabaldón, T., Martin, T., Marcet-Houben, M., Durrens, P., Bolotin-Fukuhara, M., Lespinet, O., Arnaise, S., Boisnard, S., Aguileta, G., Atanasova, R., Bouchier, C., Couloux, A., Creno, S., Almeida Cruz, J., Devillers, H., Enache-Angoulvant, A., Guitard, J., Jaouen, L., Ma, L., Marck, C., Neuvéglise, C., Pelletier, E., Pinard, A., Poulain, J., Recoquillay, J., Westhof, E., Wincker, P., Dujon, B., Hennequin, C., Fairhead, C., 2013. Comparative genomics of emerging pathogens in the Candida glabrata clade. BMC Genomics 14 (1), 623. https://doi.org/10.1186/1471-2164-14-623.

Gallegos-Garcia, V., Pan, S.J., Juarez-Cepeda, J., Ramirez-Zavaleta, C.Y., Martin-del-Campo, M., Martinez-Jimenez, V., Castano, I., Cormack, B., De Las Penas, A., 2012. A novel downstream regulatory element cooperates with the silencing machinery to repress EPA1 expression in Candida glabrata. Genetics 190, 1285–1297. https://doi.org/10.1534/genetics.111.138099.

Gutiérrez-Escobedo, G., Hernández-Carreón, O., Morales-Rojano, B., Revuelta-Rodríguez, B., Vázquez-Franco, N., Castaño, I., De Las Peñas, A., 2020. Candida glabrata peroxiredoxins, Tsa1 and Tsa2, and sulfiredoxin, Srx1, protect against oxidative damage and are necessary for virulence. Fungal Genet. Biol. 135, 103287. https://doi.org/10.1016/j.fgb.2019.103287.

Gutiérrez-Escobedo, G., Orta-Zavalza, E., Castaño, I., De Las Peñas, A., 2013. Role of glutathione in the oxidative stress response in the fungal pathogen Candida glabrata. Curr. Genet. 59 (3), 91–106. https://doi.org/10.1007/s00294-013-0390-1.

Hallstrom, T.C., Moye-Rowley, W.S., 2000. Multiple signals from dysfunctional mitochondria activate the pleiotropic drug resistance pathway in Saccharomyces cerevisiae. J. Biol. Chem. 275 (48), 37347–37356. https://doi.org/10.1074/jbc.M007338200.

Haring, M., Offermann, S., Danker, T., Horst, I., Peterhansel, C., Stam, M., 2007. Chromatin immunoprecipitation: Optimization, quantitative analysis and data normalization. Plant Methods 3, 1–16. https://doi.org/10.1186/1746-4811-3-11.

Herrero, E., 2005. Evolutionary relationships between Saccharomyces cerevisiae and other fungal species as determined from genome comparisons. Rev. Iberoam. Micol. 22 (4), 217–222. https://doi.org/10.1016/S1130-1406(05)70046-2.

Higgins, D.G., Thompson, J.D., Gibson, T.J., 1996. [22] Using CLUSTAL for multiple sequence alignments. Methods Enzymol. 383–402. https://doi.org/10.1016/S0076-6879(96)66024-8.

Huerta-Cepas, J., Capella-Gutiérrez, S., Pryszcz, L.P., Denisov, I., Kormes, D., Marcet-houben, M., Gabaldon, T., 2011. PhylomeDB v3.0 : an expanding repository of genome-wide collections of trees, alignments and phylogeny-based orthology and paralogy predictions. 39, 556–560. DOI: 10.1093/nar/gkq1109.

Juárez-Cepeda, J., Orta-Zavalza, E., Cañas-Villamar, I., Arreola-Gómez, J., Pérez-Cornejo, G.P., Hernández-Carballo, C.Y., Gutiérrez-Escobedo, G., Castaño, I., De Las Peñas, A., 2015. The EPA2 adhesin encoding gene is responsive to oxidative stress in the opportunistic fungal pathogen Candida glabrata. Curr. Genet. 61 (4), 529–544. https://doi.org/10.1007/s00294-015-0473-2.

Kalyaanamoorthy, S., Minh, B.Q., Wong, T.K.F., von Haeseler, A., Jermiin, L.S., 2017. ModelFinder: fast model selection for accurate phylogenetic estimates. Nat. Methods 14 (6), 587–589. https://doi.org/10.1038/nmeth.4285.

Khakhina, S., Simonicova, L., Moye-Rowley, W.S., 2018. Positive autoregulation and repression of transactivation are key regulatory features of the Candida glabrata Pdr1 transcription factor. Mol. Microbiol. 107 (6), 747–764. https://doi.org/10.1111/mmi.13913.

Kraneveld, E.A., de Soet, J.J., Deng, D.M., Dekker, H.L., de Koster, C.G., Klis, F.M., Crielaard, W., de Groot, P.W.J., 2011. Identification and differential gene expression of Adhesin-like wall proteins in Candida glabrata Biofilms. Mycopathologia 172 (6), 415–427. https://doi.org/10.1007/s11046-011-9446-2.

Kumar, S., Stecher, G., Tamura, K., 2016. MEGA7: molecular evolutionary genetics analysis Version 7.0 for bigger datasets. Mol. Biol. Evol. 33, 1870–1874. https://doi.org/10.1093/molbev/msw054.

Kurtzman, C.P., 2003. Phylogenetic circumscription of Saccharomyces, Kluyveromyces and other members of the Saccharomycetaceae, and the proposal of the new genera Lachancea, Nakaseomyces, Naumovia, Vanderwaltozyma and Zygotorulaspora. FEMS Yeast Res. 4, 233–245. https://doi.org/10.1016/S1567-1356(03)00175-2.

Lacazette, E., 2017. A laboratory practical illustrating the use of the ChIP-qPCR method in a robust model: Estrogen receptor alpha immunoprecipitation using Mcf-7 culture cells. Biochem. Mol. Biol. Educ. 45 (2), 152–160. https://doi.org/10.1002/bmb.20999.

Lamping, E., Baret, P.V., Holmes, A.R., Monk, B.C., Goffeau, A., Cannon, R.D., 2010. Fungal PDR transporters: Phylogeny, topology, motifs and function. Fungal Genet. Biol. 47 (2), 127–142. https://doi.org/10.1016/j.fgb.2009.10.007.

Larkin, M.A., Blackshields, G., Brown, N.P., Chenna, R., McGettigan, P.A., McWilliam, H., Valentin, F., Wallace, I.M., Wilm, A., Lopez, R., Thompson, J.D., Gibson, T.J., Higgins, D.G., 2007. Clustal W and Clustal X version 2.0. Bioinformatics 23 (21), 2947–2948. https://doi.org/10.1093/bioinformatics/btm404.

Leiva-Peláez, O., Gutiérrez-Escobedo, G., López-Fuentes, E., Cruz-Mora, J., De Las Peñas, A., Castaño, I., 2018. Molecular characterization of the silencing complex SIR in Candida glabrata hyperadherent clinical isolates. Fungal Genet. Biol. 118, 21–31. https://doi.org/10.1016/j.fgb.2018.05.005.

López-Fuentes, E., Hernández-Hernández, G., Castanedo, L., Gutiérrez-Escobedo, G., Oktaba, K., De las Peñas, A., Castaño, I., 2018. Chromatin loop formation induced by a subtelomeric protosilencer represses EPA genes in Candida glabrata. Genetics 210, 113–128. DOI: 10.1534/genetics.118.301202.

Ma, B., Pan, S.-J., Domergue, R., Rigby, T., Whiteway, M., Johnson, D., Cormack, B.P., 2009. High-affinity transporters for NAD+ precursors in Candida glabrata are regulated by Hst1 and induced in response to niacin limitation. Mol. Cell. Biol. 29 (15), 4067–4079. https://doi.org/10.1128/MCB.01461-08.

Martínez-Jiménez, V., Ramírez-Zavaleta, C.Y., Orta-Zavalza, E., Díaz de León, G., Gutiérrez-Escobedo, G., Ponce de León, A., Sifuentes-Osornio, J., Bobadilla del Valle, M., De Las Peñas, A., Castaño, I., 2013. Sir3 Polymorphisms in Candida glabrata Clinical Isolates. Mycopathologia 175 (3-4), 207–219. https://doi.org/10.1007/s11046-013-9627-2.

Minh, B.Q., Nguyen, M.A.T., von Haeseler, A., 2013. Ultrafast approximation for phylogenetic bootstrap. Mol. Biol. Evol. 30 (5), 1188–1195. https://doi.org/10.1093/molbev/mst024.

Morschhäuser, J., 2010. Regulation of multidrug resistance in pathogenic fungi. Fungal Genet. Biol. 47 (2), 94–106. https://doi.org/10.1016/j.fgb.2009.08.002.

Moye-Rowley, W.S., 2019. Multiple interfaces control activity of the Candida glabrata Pdr1 transcription factor mediating azole drug resistance. Curr. Genet. 65 (1), 103–108. https://doi.org/10.1007/s00294-018-0870-4.

Noble, J.A., Tsai, H.-F., Suffis, S.D., Su, Q., Myers, T.G., Bennett, J.E., 2013. STB5 is a negative regulator of azole resistance in Candida glabrata. Antimicrob. Agents Chemother. 57 (2), 959–967. https://doi.org/10.1128/AAC.01278-12.

Orta-Zavalza, E., Guerrero-Serrano, G., Gutiérrez-Escobedo, G., Cañas-Villamar, I., Juárez-Cepeda, J., Castaño, I., De Las Peñas, A., 2013. Local silencing controls the oxidative stress response and the multidrug resistance in Candida glabrata. Mol. Microbiol. 88 (6), 1135–1148. https://doi.org/10.1111/mmi.12247.

Pak, J., Segall, J., 2002. Regulation of the premiddle and middle phases of expression of the NDT80 gene during sporulation of Saccharomyces cerevisiae. Mol. Cell. Biol. 22 (18), 6417–6429. https://doi.org/10.1128/MCB.22.18.6417-6429.2002.

Paul, S., McDonald, W.H., Moye-Rowley, W.S., 2018. Negative regulation of Candida glabrata Pdr1 by the deubiquitinase subunit Bre5 occurs in a ubiquitin independent manner. Mol. Microbiol. 110 (2), 309–323. https://doi.org/10.1111/mmi.14109.

Paul, S., Moye-Rowley, W.S., 2014. Multidrug resistance in fungi: regulation of transporter-encoding gene expression. Front. Physiol. 5, 1–14. https://doi.org/10.3389/fphys.2014.00143.

Pfaller, M.A., Andes, D.R., Diekema, D.J., Horn, D.L., Reboli, A.C., Rotstein, C., Franks, B., Azie, N.E., Chauhan, N., 2014. Epidemiology and outcomes of invasive candidiasis due to non-albicans species of Candida in 2,496 patients: Data from the Prospective Antifungal Therapy (PATH) registry 2004–2008. PLoS One 9 (7), e101510. https://doi.org/10.1371/journal.pone.0101510.

Piekarska, I., Rytka, J., Rempola, B., 2010. Regulation of sporulation in the yeast Saccharomyces cerevisiae. Acta Biochim. Pol. 57 (3) https://doi.org/10.18388/abp.2010_2401.

Pierce, M., Benjamin, K.R., Montano, S.P., Georgiadis, M.M., Winter, E., Vershon, A.K., 2003. Sum1 and Ndt80 Proteins Compete for Binding to Middle Sporulation Element Sequences That Control Meiotic. Gene Expression 23, 4814–4825. https://doi.org/10.1128/MCB.23.14.4814.

Redding, S.W., Kirkpatrick, W.R., Saville, S., Coco, B.J., White, W., Fothergill, A., Rinaldi, M., Eng, T., Patterson, T.F., Lopez-ribot, J., 2003. Multiple Patterns of Resistance to Fluconazole in. Microbiology 41, 619–622. https://doi.org/10.1128/JCM.41.2.619.

Roetzer, A., Gratz, N., Kovarik, P., SchÃ¼ller, C., 2010. Autophagy supports Candida glabrata survival during phagocytosis. Cell. Microbiol. 12, 199–216. DOI: 10.1111/j.1462-5822.2009.01391.x.

Roetzer, A., Klopf, E., Gratz, N., Marcet-Houben, M., Hiller, E., Rupp, S., Gabaldón, T., Kovarik, P., Schüller, C., 2011. Regulation of Candida glabrata oxidative stress resistance is adapted to host environment. FEBS Lett. 585, 319–327. https://doi.org/10.1016/j.febslet.2010.12.006.

Saijo, T., Miyazaki, T., Izumikawa, K., Mihara, T., Takazono, T., Kosai, K., Imamura, Y., Seki, M., Kakeya, H., Yamamoto, Y., Yanagihara, K., Kohno, S., 2010. Skn7p is involved in oxidative stress response and virulence of Candida glabrata. Mycopathologia 169 (2), 81–90. https://doi.org/10.1007/s11046-009-9233-5.

Sanglard, D., Ischer, F., Calabrese, D., Majcherczyk, P.A., Bille, J., 1999. The ATP binding cassette transporter gene CgCDR1 from Candida glabrata is involved in the resistance of clinical isolates to azole antifungal agents. Antimicrob. Agents Chemother. 43, 2753–65. DOI: 10.1128/AAC.43.11.2753.

Seider, K., Brunke, S., Schild, L., Jablonowski, N., Wilson, D., Majer, O., Barz, D., Haas, A., Kuchler, K., Schaller, M., Hube, B., 2011. The Facultative Intracellular Pathogen Candida glabrata Subverts Macrophage Cytokine Production and Phagolysosome Maturation. J. Immunol. 187 (6), 3072–3086. https://doi.org/10.4049/jimmunol.1003730.

Seider, K., Gerwien, F., Kasper, L., Allert, S., Brunke, S., Jablonowski, N., Schwarzmüller, T., Barz, D., Rupp, S., Kuchler, K., Hube, B., 2014. Immune evasion, stress resistance, and efficient nutrient acquisition are crucial for intracellular survival of Candida glabrata within macrophages. Eukaryot. Cell 13 (1), 170–183. https://doi.org/10.1128/EC.00262-13.

Sikorski, R.S., Hieter, P., 1989. A system of shuttle vectors and yeast host strains designed for efficient manipulation of DNA in Saccharomyces cerevisiae. Genetics 122, 19–27. https://doi.org/10.1093/genetics/122.1.19.

Skrzypek, M.S., Binkley, J., Binkley, G., Miyasato, S.R., Simison, M., Sherlock, G., 2017. The Candida Genome Database (CGD): Incorporation of Assembly 22, systematic identifiers and visualization of high throughput sequencing data. Nucleic Acids Res. 45 (D1), D592–D596. https://doi.org/10.1093/nar/gkw924.

Thakur, J.K., Arthanari, H., Yang, F., Pan, S.-J., Fan, X., Breger, J., Frueh, D.P., Gulshan, K., Li, D.K., Mylonakis, E., Struhl, K., Moye-Rowley, W.S., Cormack, B.P., Wagner, G., Näär, A.M., 2008. A nuclear receptor-like pathway regulating multidrug resistance in fungi. Nature 452 (7187), 604–609. https://doi.org/10.1038/nature06836.

Timmermans, B., De Las Peñas, A., Castaño, I., Van Dijck, P., 2018. Adhesins in Candida glabrata. J. Fungi 4 (2), 60. https://doi.org/10.3390/jof4020060.

Trifinopoulos, J., Nguyen, L., Haeseler, A. Von, Minh, B.Q., 2016. W-IQ-TREE : a fast online phylogenetic tool for maximum likelihood analysis 44, 232–235. DOI: 10.1093/nar/gkw256.

Tsai, H.-F., Krol, A.A., Sarti, K.E., Bennett, J.E., 2006. Candida glabrata PDR1, a transcriptional regulator of a pleiotropic drug resistance network, mediates azole resistance in clinical isolates and petite mutants. Antimicrob. Agents Chemother. 50 (4), 1384–1392. https://doi.org/10.1128/AAC.50.4.1384-1392.2006.

Vale-Silva, L., Ischer, F., Leibundgut-Landmann, S., Sanglard, D., Deepe, G.S., 2013. Gain-of-function mutations in PDR1, a regulator of antifungal drug resistance in candida glabrata, control adherence to host cells. Infect. Immun. 81 (5), 1709–1720. https://doi.org/10.1128/IAI.00074-13.

Vale-Silva, L.A., Moeckli, B., Torelli, R., Posteraro, B., Sanguinetti, M., Sanglard, D., 2016. Upregulation of the Adhesin Gene EPA1 Mediated by PDR1 in Candida glabrata Leads to Enhanced Host Colonization. mSphere 1, 1–16. DOI: 10.1128/mSphere.00065-15.

Vermitsky, J.-P., Earhart, K.D., Smith, W.L., Homayouni, R., Edlind, T.D., Rogers, P.D., 2006. Pdr1 regulates multidrug resistance in Candida glabrata: gene disruption and genome-wide expression studies. Mol. Microbiol. 61 (3), 704–722. https://doi.org/10.1111/j.1365-2958.2006.05235.x.

Whaley, S.G., Caudle, K.E., Simonicova, L., Zhang, Q., Moye-Rowley, W.S., Rogers, P.D., 2018. Jjj1 Is a Negative Regulator of Pdr1-Mediated Fluconazole Resistance in Candida glabrata. mSphere 3, 1–11. DOI: 10.1128/msphere.00466-17.

Whaley, S.G., Rogers, P.D., 2016. Azole resistance in Candida glabrata. Curr. Infect. Dis. Rep. 18, 41. https://doi.org/10.1007/s11908-016-0554-5.